The Planetary Science Journal, 6:173 (37pp), 2025 July https://doi.org/10.3847/PSJ/ade786

Simulating Science Operations for a Joint Rover-helicopter Mission Architecture in a Mars Analog Setting

Kathryn M. Stack[1], Raymond Francis[1], Fred J. Calef, III[1], Samantha J. Gwizd[1], Jeffrey F. Schroeder[1], Joana R. C. Voigt[1], Thorsteinn Kristinsson[2,3], Peter Schroedl[4], Jahnavi Shah[5,6], Matthew Varnam[7,8], Catherine D. Neish[5], Reid P. Perkins[5], Sashank Vanga[5], Michael S. Bramble[1], Andrea Donnellan[1], Jeffrey T. Osterhout[1], Michael Tuite[1], Brett B. Carr[7], and Christopher W. Hamilton[7]

[1] Jet Propulsion Laboratory, California Institute of Technology, Pasadena, CA 91109, USA; kathryn.m.stack@jpl.nasa.gov
[2] Purdue University, West Lafayette, IN 47907, USA
[3] University of Colorado Boulder, Boulder, CO 80309, USA
[4] Boston University, Boston, MA 02215, USA
[5] Western University, London, ON N6A 3K7, Canada
[6] Queens University, Kingston, ON K7L 3N6, Canada
[7] Lunar and Planetary Laboratory, University of Arizona, Tucson, AZ 85721, USA
[8] The University of Edinburgh, Edinburgh, Scotland, EH8 9YL, UK
Received 2024 November 1; revised 2025 June 17; accepted 2025 June 20; published 2025 July 22

Abstract

Aerial platforms can explore planetary surfaces without the mobility limitations of rovers and landers. Inspired by the recent successes and challenges of NASA's IngenuAity Mars Helicopter, the Rover-Aerial Vehicle Exploration Network project explored the operations and science value of a dual-platform rover-helicopter mission architecture coupled with simulated orbiter image data. A remote mission operations team carried out a 5 day long Mars mission simulation executed by a field team in the Rainbow Basin Natural Area near Barstow, California, USA. The simulation demonstrated the rover's ability to collect progressively finer-scale, specifically targeted image and compositional observations with a complementary multi-instrument payload. The helicopter excelled at the collection of extensive image surveys, providing views of diverse terrains and geologic units within the exploration area otherwise inaccessible to the rover. Of the helicopter data, high-resolution, low-altitude oblique images proved to be the most useful from a science and strategic operational planning perspective. The dual-platform mission architecture had clear science advantages over the individual rover or helicopter investigations during the simulation, but sharing daily data downlink between the mission platforms presented one of the greatest operational challenges. Rover operations demanded daily "reactive" tactical planning and rapid downlink of science data to enable targeting and traverse decisions, while the helicopter was best suited to a "predictive" advanced planning timeline for operations, data volume management, and science analysis.

Unified Astronomy Thesaurus concepts: Mars (1007); Planetary geology (2288); Geological processes (2289); Planetary science (1255)

1. Introduction

Over the past decade, there has been increased recognition of the value of rotorcraft for exploring planetary surfaces, particularly compared to conventional landers and rovers (e.g., J. Bapst et al. 2021). Rotorcraft are lightweight, relatively inexpensive, and can access more hazardous terrains and distant targets than a typical rover (J. Bapst et al. 2021). They can also be used to generate high-resolution, three-dimensional models or image and multispectral data for planetary surfaces (e.g., K. M. Bateman et al. 2022; B. B. Carr et al. 2024; G. R. Kodikara et al. 2024). NASA's Ingenuity Mars Helicopter (J. Balaram et al. 2021), which executed 72 flights as part of the Mars 2020 mission, introduced powered, controlled flight as a novel mode of planetary exploration (T. Tzanetos et al. 2022). The Dragonfly rotorcraft (J. W. Barnes et al. 2021), set to explore Saturn's moon Titan in the mid-2030s, will continue to advance aerial exploration of planetary bodies within the solar system, while mission concepts for stand-alone Mars helicopter missions are currently in development (J. Bapst et al. 2021; L. A. Young et al. 2021; S. Withrow-Maser et al. 2021).

Ingenuity's Technology and Operations Demonstrations provided proof of concept that a helicopter could aid in the robotic operation and science mission of a rover (T. Tzanetos et al. 2022). However, the helicopter's safe landing limitations and its preference for a line-of-sight telecommunications link with the Perseverance rover for receipt of command sequences and transmission of data (e.g., F. Alibay et al. 2022) at times constrained and impacted the operation of both helicopter and rover (J. L. Anderson et al. 2024). As a technology demonstration, Ingenuity was operated with limited representation and integration with the Perseverance Science Team (F. Alibay et al. 2022; J. L. Anderson et al. 2023) given the Science Team's prioritization of the rover's science and sampling objectives.

The value of stand-alone rover and helicopter missions has been demonstrated both on the surface of Mars and in a variety of field analog tests carried out on Earth (e.g., R. A. Yingst et al. 2016, 2020, 2022; G. R. Osinski et al. 2019; B. B. Carr et al. 2024; S. Gwizd et al. 2024; G. R. Kodikara et al. 2024),

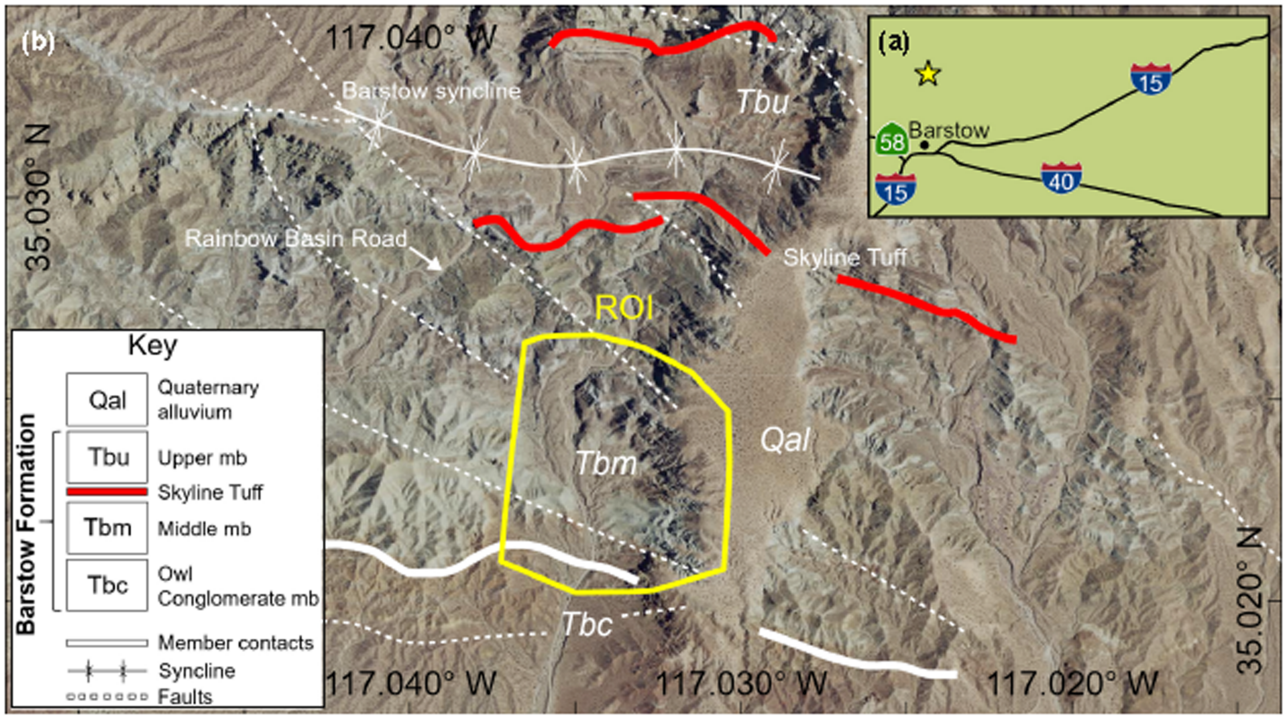

Figure 1. Mission simulation field site at the Rainbow Basin Natural Area near Barstow, California, USA. (a) Rainbow Basin Natural Area (yellow star) relative to the city of Barstow and nearby major highways. (b) The region of interest (ROI, outlined in yellow) explored in this simulation overlaid on the major geologic units and structures within Rainbow Basin after N. P. Lang et al. (2011). Image basemap credit: Copernicus Sentinel-2 provided by EOX IT.

but the successes and challenges of the Ingenuity operations demonstration on Mars motivate further exploration of dual-platform mission architectures. A joint rover-helicopter mission architecture in which the platforms are fully integrated and of equal mission priority, but with both shared and distinct science and operational objectives, would require a synergistic concept beyond that explored and implemented by the Ingenuity operations demonstration. Considerations for such a dual-platform mission would include allocation of mission resources (e.g., plan duration, available energy, downlink data volume), coordination and balance of the rover and helicopter's respective individual versus shared science and operational objectives, and the operational planning processes, roles, and timelines required for each mission platform. Evaluating such a mission architecture would also provide an opportunity for direct comparison between the science value and operational efficacy of stand-alone rover, stand-alone helicopter, and combined mission architectures, respectively, at the same exploration site.

With the goal of designing, developing, and practicing rover and helicopter science operations for a realistic joint rover-helicopter mission on Mars, the Rover-Aerial Vehicle Exploration Network (RAVEN; C. W. Hamilton et al. 2023) designed and executed a 5 sol (Martian day) mission simulation on 2023 November 6–10, in the Rainbow Basin Natural Area near Barstow, California, USA (Figure 1). Building on the RAVEN project's previous stand-alone rover (S. Gwizd et al. 2024) and helicopter (B. B. Carr et al. 2024) field mission simulations, a remote mission operations team and a field implementation team simulated the joint science operations of a Curiosity/Perseverance-class Mars rover and a helicopter with some enhanced capabilities compared to Ingenuity. High-resolution orbiter image data like those provided by the Mars Reconnaissance Orbiter High Resolution Imaging Science Experiment (HiRISE; A. S. McEwen et al. 2007) were also simulated to enable strategic science mission planning prior to and during the simulation. Specific objectives of this simulation included (1) evaluating the science value and return of a joint rover-helicopter mission compared to stand-alone rover and helicopter missions; (2) evaluating the optimization and balance of science objectives of each platform (i.e., rover or helicopter) in a dual-platform architecture; (3) identifying and exploring the operational impact and dependencies of the rover and helicopter on each other in a dual-platform scenario; and (4) understanding the science value and resource cost of using the helicopter to aid in traverse planning and enhanced localization of the rover. This paper describes the design and development of this simulated joint rover-helicopter mission, provides a summary of the mission simulation as conducted, and discusses lessons learned and implications of the simulation for joint and individual rover and helicopter science operations on Mars.

2. Mission Simulation Design

To simulate a joint rover-helicopter mission, a team of nine scientists worked via remote video conference to build (1) a strategic science plan using simulated orbiter data of the mission's region of interest (ROI) that informed the construction of (2) daily activity plans during a 5 day long mission (Sols 101–105) involving rover and helicopter operations. The simulation included "responsive" field data from a field site for Sols 101–105, meaning a five-person field team collected data to simulate each observation requested by the mission operations team. The location of this field site was unknown to the remote mission operations team before and during the 5 day mission simulation. The field team employed a strategy successfully used in previous field analog activities (J. E. Moores et al. 2012; R. Francis et al. 2018; G. R. Osinski et al. 2019; S. Gwizd et al. 2024) for simulating planetary robotic and science

operations and instrument observations with handheld field instrumentation. At the conclusion of the 5 day simulation, the remote mission operations team constructed a high-level plan for an additional five sols of activities (Sols 106–110). Field data were not collected for Sols 106–110.

Given the limited 5 day duration of the simulation, only a single exploration scenario for the joint rover-helicopter mission was carried out. This was an intentional simulation design decision to prioritize high-fidelity daily operations processes, science discussions, and decision-making on a realistic mission timeline, and a response to realistic field data in favor of attempting multiple mission exploration scenarios with lower-fidelity science decision-making, timelines, and processes. Operational constraints related to the simulation's duration are discussed in the following two sections, and the implications of these constraints on the simulation are discussed in Section 5.5.

2.1. Mission Operations

The operational design, roles, and procedures of this mission simulation were based off those used for the Mars Exploration Spirit and Opportunity (A. H. Mishkin et al. 2006), Mars Science Laboratory (MSL) Curiosity (A. R. Vasavada 2022), and the Mars 2020 Perseverance rover missions (S. M. Milkovich et al. 2022), with Mars 2020 operations processes serving as the main inspiration for the science activities and activity plan structure used in the simulation (see Appendix A). The operations design of the simulation was specifically adapted from S. Gwizd et al. (2024) for use in this dual-platform mission scenario, the details of which can be found in Appendix A. Following the operations process design described in S. Gwizd et al. (2024), this simulation's mission planning took place over four different timescales: strategic (weeks to months), tactical (daily "N" planning, where N is the number of the sol currently being planned and the next to be carried out by the mission), next day ("$N + 1$" planning), and near-term ("$N + 2$" to "$N + 7$" planning) (Appendix A). Strategic planning was carried out 1–2 months prior to the start of the mission simulation and was inspired by the strategic planning process implemented by the Perseverance rover team (V. Z. Sun et al. 2024), while the tactical, next day, and near-term planning processes were carried out or managed daily during the five days of the mission simulation. Although this simulation incorporated some aspects of engineering operations (e.g., resource management) and robotic operations (e.g., adhering to safety constraints when planning rover traverse and helicopter flight paths), simulating high-fidelity science operations and science decision-making was the main priority and a full simulation of engineering and robotic operations was considered out of scope.

2.2. Field Site and Simulated Science Scenario

The field site used in this simulation was the Rainbow Basin Natural Area, a National Natural Landmark and an Area of Critical Environmental Concern managed by the Bureau of Land Management. Rainbow Basin is situated 13.8 km north of the city of Barstow within the Mud Hills range of the northwestern Mojave Desert in San Bernadino County, California, USA (Figure 1). Rainbow Basin primarily comprises sedimentary, volcanic, and volcaniclastic deposits of the Miocene-aged (ca. 19–13 Ma) Barstow Formation (T. W. Diblee 1968; M. O. Woodburne et al. 1990). Since distinguishing between fluvial, lacustrine, and volcaniclastic deposits can be challenging on Mars (e.g., K. S. Edgett & R. Sarkar 2021), Rainbow Basin and the Barstow formation provide a valuable planetary exploration analog (N. P. Lang et al. 2011) in which to field test rover and helicopter science operations.

The mission operations team identified three primary science goals to guide the selection and prioritization of planned activities for the rover and helicopter during the mission simulation. Goals were to (1) characterize the geology of the mission exploration area; (2) assess the rock record's habitability and potential for preserving ancient biosignatures; and (3) characterize past climatic conditions. At the start of the simulation, the remote operations team was given the following additional high-level mission guidelines: (1) both the rover and helicopter would progress approximately south to north through the ROI; (2) the team was to look for a compelling outcrop in the southern part of the ROI at which the rover could deploy its full instrument payload during the five sols of the simulation; (3) the team could assume that a second stop for detailed rover science would occur in the northern part of the ROI sometime in the week(s) following the 5 sols of the simulation; and (4) the team should consider how the helicopter could be used to both scout ahead for the rover and contribute independently toward accomplishing the mission's science goals. The requirement for the rover to deploy its full instrument payload at least once during the mission simulation decreased the team's flexibility to develop a fully discovery-driven mission plan for the rover and the helicopter. However, this choice enabled a better comparison of the science contribution and potential value of the rover and helicopter payloads, respectively.

2.3. Simulated Mission Platforms

The simulated mission involved a Curiosity/Perseverance-class rover with analogous mobility and science payload capabilities in joint operation with an Ingenuity-class helicopter with enhanced landing, telecommunications, and science capabilities compared to Ingenuity. The simulation also involved images of the field area simulating those provided by an orbiter camera such as HiRISE.

2.3.1. Orbiter

The mission operations team was provided with analog HiRISE data products derived from an unoccupied aircraft system (UAS) imaging survey of Rainbow Basin acquired in 2018 with a GoPro HERO6 Black mounted under a 3DRobotics Solo UAS (Figures 2 and B1). The original UAS orthomosaic was down-sampled to 25 cm pixel^{-1} and the coreferenced digital elevation model (DEM) to 1 m pixel^{-1}, which are, respectively, the equivalent pixel scale for the best HiRISE data used for Mars surface mission basemaps (e.g., R. L. Fergason et al. 2020). The analog HiRISE orthomosaic was also modified to minimize evidence of obvious human-made structures (e.g., blurring of the road that bisected the field area (Figure B1(b))). The elevation data were processed to generate a slope map using Horn's method (B. K. P. Horn 1981) for evaluating rover traversability (Figure B1(d)).

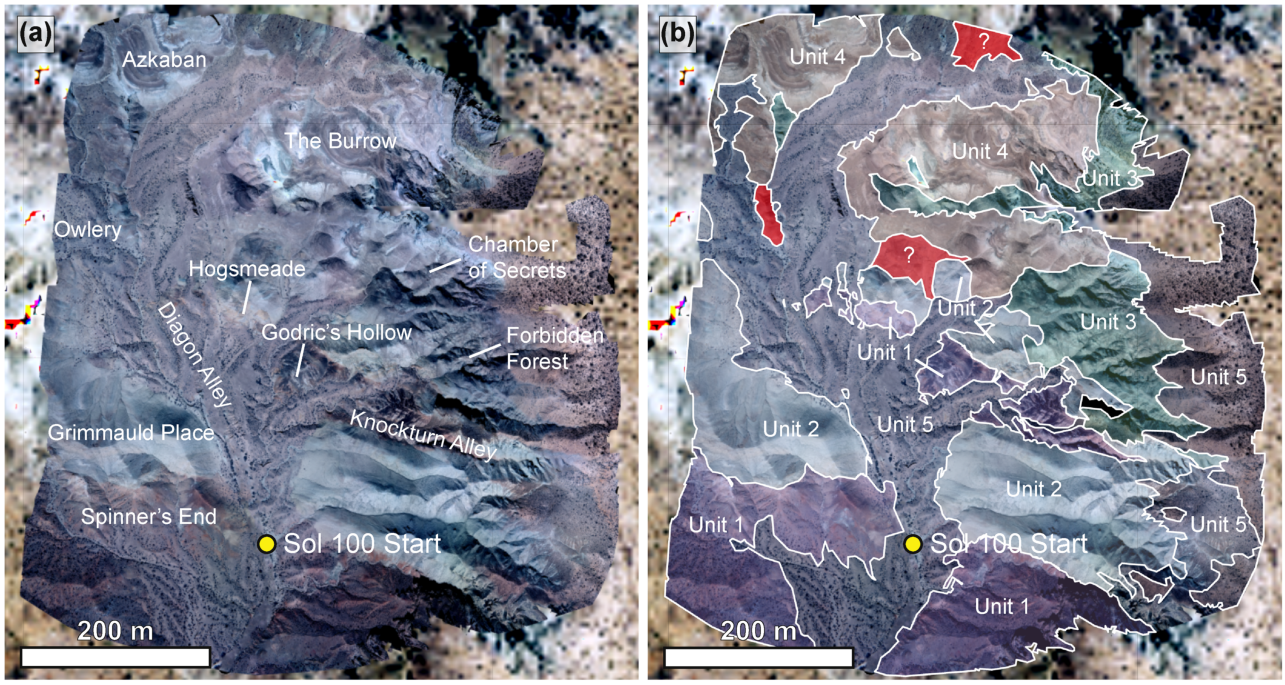

Figure 2. Informal landmark names and the photogeologic map constructed for the ROI during strategic planning. (a) Analog orbiter orthomosaic basemap at HiRISE-equivalent resolution (25 cm pixel^{-1}) showing the major informally named landmarks of the mission simulation. (b) Geologic units mapped in the ROI based on differences in color, morphology, and weathering style observed in the analog HIRISE basemap.

2.3.2. Rover

The simulated rover was assumed to have a maximum daily traverse limit of 100 m, which is less than the maximum distance of ∼350 m traversed by Perseverance in a single sol (V. Verma et al. 2023), but closer to an average daily traverse distance across variable terrain types assuming a mix of autonomous and directed drives (V. Verma et al. 2023). The simulated rover was constrained to traversing slopes <30°, consistent with Curiosity's slope tolerance during drives (M. Heverly et al. 2013) and for the safety of the field team. The simulated rover was assumed to have a Perseverance-like autonavigation capability (V. Verma et al. 2023) such that a designated end-of-drive target at the end of a 100 m drive could be achieved within an error radius of ∼5 m (V. Verma et al. 2024). To explore the potential of helicopter image data to improve the efficiency of rover driving, an "enhanced localization" capability was simulated whereby the rover's positional uncertainty after a long drive could be decreased to zero if a low-altitude helicopter image survey had been acquired and downlinked (returned to Earth) over the last ∼30 m of a future rover drive before it was planned. This "enhanced localization" capability assumed only that the low-altitude helicopter survey images could be transmitted to Earth from the helicopter via an orbiter in accordance with the mission's data downlink constraints (see Section 2.3.4.), that these images were sufficient for engineers on Earth to create hazard maps and identify keep-out zones and localization tie points, and that the rover would be capable of uplinking these engineering data products and processing them during driving (e.g., V. Verma et al. 2023). This hazard analysis was assumed to have been performed by engineers on Earth but was not actually performed during the simulation since high-fidelity robotic operations were not in scope. This capability did not require assumptions regarding helicopter computing capabilities beyond a telecommunications link with an orbiter or rover processing capabilities beyond those of Perseverance.

The instrument suite simulated on the rover's remote-sensing mast and robotic arm turret were inspired by the instrument payloads of the Curiosity and Perseverance rovers (Table 1). In this simulation, use of the rover's mast instruments was referred to as "remote sensing" science, while use of the rover's arm turret instruments was referred to as "proximity science," as it is on Mars 2020 (e.g., V. Z. Sun et al. 2023). The rover was assumed to have a limited autonomous targeting capability, analogous to the Autonomous Exploration for Gathering Increased Science (AEGIS) algorithm in use by the Curiosity and Perseverance rovers (R. Francis et al. 2017). It was assumed that the rover had some capability for abrasion or dust removal from a natural outcrop surface, although the field team did not simulate abrasion in the field to avoid physical damage to the outcrop.

2.3.3. Helicopter

The helicopter simulated in this mission was based on the Ingenuity helicopter (J. Balaram et al. 2021), with several modifications. It was assumed that this simulation's helicopter had a maximum single-sol flight range of 300 m, just above the average flight distance flown by Ingenuity during flights 3–13 (T. Tzanetos et al. 2022). Unlike Ingenuity, which typically required line-of-sight communication with the Perseverance rover (H. F. Grip et al. 2022), this simulation assumed a helicopter capable of independent telecommunications with an orbiter. It was also assumed that the helicopter would have onboard autonomous landing capability (e.g., R. Brockers et al. 2022), and a maximum slope of 10° for its landing areas, an increase from Ingenuity's <5° requirement (J. Balaram et al. 2021). This simulation did not assume a slope constraint for the helicopter flight path. The field team introduced an

Table 1
Simulated Rover and Helicopter Science Payloads

Mission	Position	Mission Simulation Instrument/ Capability	MSL/M2020 Comparable Instrument	Description	Citation	Simulation Field Instrument
Rover	Rover remote-sensing mast	Navcam	NavCam	Color camera providing context for targeting and traverse planning	J. Maki et al. (2012, 2020)	Tripod-mounted DSLR monocular camera
		Mastcam	Mastcam/Mastcam-Z	Color camera used to image landscape-to-outcrop-scale features	J. F. Bell et al. (2017, 2021)	Tripod-mounted DSLR monocular camera (images cropped to approximate instrument field of view, FOV
		RMI	ChemCam/Supercam RMI	Color telescopic camera providing context for targeting and for imaging millimeter- to centimeter-scale features	S. Maurice et al. (2012, 2021)	Tripod-mounted DSLR monocular camera (images cropped to approximate instrument FOV)
		VISIR	Supercam IR	Infrared wavelength (1.3–2.6 μm) spectrometer	S. Maurice et al. (2021)	ASD FieldSpec 4 Hi-Res spectroradiometer (spatial resolution = 8 nm)
		LIBS	ChemCam/Supercam LIBS	500 μm spot size laser-induced breakdown spectrometer	S. Maurice et al. (2012, 2021)	SciAPS Z300 LIBS handheld field instrument (wavelength range = 190–950 nm)
	Rover arm	Turretcam	MAHLI/WATSON	Color camera used to image micrometer- to centimeter-scale features	K. S. Edgett et al. (2012); R. Bhartia et al. (2021)	Handheld digital SLR monocular camera (images cropped to approximate instrument FOV)
		XRF	APXS/PIXL	X-ray fluorescence spectrometer providing bulk elemental composition	R. Gellert & B. C. Clark (2015); A. C. Allwood et al (2020)	Handheld XRF SciAps X-300 Analyzer spectrometer
		RAMAN	SHERLOC	Raman spectrometer	R. Bhartia et al. (2021)	Handheld dual laser (785 and 852 cm^{-1}) BRUKER BRAVO field Raman spectrometer
Helicopter	Underside of helicopter	High-altitude survey imaging (nadir)	Return to Earth (RTE) Camera	Color camera providing nadir and oblique color images of the surface as the helicopter hovers several meters above the ground, and fixed-focus images while landed	J. Balaram et al. (2021); J. Maki et al. (2024)	GoPro HERO6 Black on a remotely piloted 3DRobotics Solo small UAS
		Low-altitude survey imaging (nadir)				
		Oblique imaging				Samsung Galaxy SM-G991U camera on a stick
		Landed imaging (nadir)				Tripod-mounted digital SLR monocular camera
		VISIR	N/A	Infrared wavelength (1.3–2.6 μm) spectrometer	N/A	ASD FieldSpec 4 Hi-Res spectroradiometer (spatial resolution = 8 nm)

∼5 m radius error on helicopter landing sites, a significant improvement on Ingenuity's <13% positional uncertainty error (V. Verma et al. 2024).

Table 1 lists the helicopter's simulated payload. It was an intentional choice to limit the helicopter's science payload compared to the rover's, in line with the mass constraints for aerial science payloads (i.e., less than several kilograms; S. Withrow-Maser et al. 2021). The helicopter's nadir fixed-position survey color imager was simulated to have a low-altitude survey mode (10 m above ground level) with a spatial resolution of 3 cm pixel^{-1} and swath width of 24.5 m, and a high-altitude survey mode (20 m above ground level) at a resolution of 6 cm pixel^{-1} and swath width of 49 m. The nadir-looking survey camera data were simulated with images from a data set collected by a UAS for a previous field campaign in 2018 (Appendix B, Figure B1). During processing, several color artifacts, e.g., a tan outcrop changing abruptly to a red outcrop, were introduced into the orthomosaic due to changes in lighting conditions or camera settings during the camera survey. The simulated oblique low-altitude color imager acquired images ∼5 m above ground level with an instantaneous field of view (or iFOV) ∼0.3 mrad pixel^{-1} and FOV ∼70° width by ∼50° height.

2.3.4. Mission Resource Constraints

The rover and the helicopter were each given independent daily duration and energy budgets. The duration of science and engineering activities for each platform was restricted to 360 minutes. The rover's energy constraint (400 Watt-hours, Wh) was derived from a typical radioisotope thermoelectric generator (RTG)-based Curiosity/Perseverance-class mission. The helicopter was given a daily energy budget of 75 Wh assuming a solar-powered helicopter, compared to Ingenuity's 40 Wh full charge capacity (J. Balaram et al. 2021). As a given that the rover and the helicopter would be operating in the same exploration area, it was assumed that both would share orbiter overflight windows and an 1120 Mbit "decisional" downlink data volume budget. This data volume budget referred to the amount of data that could be sent from Mars and received on Earth in time to enable the next sol's planning cycle, and assumed relay support like that of the Curiosity and Perseverance rover missions (e.g., E. Young et al. 2023). Both the rover and the helicopter had the ability to acquire data on any given sol in excess of this decisional data limit, but any additional "nondecisional" data acquired would remain "on board" unless selected for downlink during a subsequent sol's decisional pass. At the end of the simulation, the mission operations team selected 60% of the remaining onboard data for downlink to simulate the contribution of nondecisional passes over several days, while the remaining 40% of data stayed on board and was not given to the mission operations team.

3. Mission Simulation

3.1. Strategic Mission Planning

Geologic mapping of the ROI during pre-mission strategic planning led to the identification of five units distinguished by color, outcrop expression, and the presence or absence of layering observed in analog orbiter images (Figure 2(b)). Unit 1 is a reddish-purple unit identified in the southern part of the ROI in two east–west-oriented exposures. Unit 2, a light-toned whitish-yellow unit, occurs between the two Unit 1 exposures. A fold axis or a fault was speculated to trend northwest–southeast through Unit 2 to explain the repetition of Unit 1. Unit 3 crops out north and east of Unit 1 and 2, and exhibits alternating brown, white, and greenish thin meter-scale layers. Unit 4, a layered unit of meter- to several meter-thick brown and tan layers alternating with thinner green layers, crops out north of Unit 3 and is prominent in the northern part of the ROI. Unit 5 includes all the alluvium throughout the ROI.

It was immediately apparent to the team upon examining the analog orbiter data that the rover would likely be limited to traversing the "Diagon Alley" corridor given the high slopes within Units 1 and 2 (Figures 2(a) and B1(d)). Although the color variations observed throughout the southern ROI implied bedrock diversity, it was difficult to confirm the presence of exposed bedrock versus scree slopes in the orbiter images. The team felt more confident that bedrock would be accessible to the rover in the "Godric's Hollow" area near the center of the ROI given the multicolored layering expressed there (Figure 2). Thus, the team developed a notional plan to prioritize this site for a proximity science investigation. Given that Godric's Hollow was over 200 m away along a reasonable traverse path from the Sol 100 starting position, it also became clear that the rover would be limited to the southern portion of the ROI during the 5 day mission simulation.

In support of the rover's traverse through Diagon Alley and its likely detailed investigation at Godric's Hollow, the team planned for the helicopter to first fly the length of the rover's planned traverse. This flight's objectives would be to scout the rover's likely exploration area during the simulation with a focus on Godric's Hollow to identify well-preserved, accessible outcrops for the rover's proximity science and to enable the rover's enhanced localization. In addition to using the helicopter to support and scout for the rover, the team developed a notional plan for the helicopter to land on or fly over each of five units identified during the team's geologic mapping effort. The team was particularly interested in using the helicopter to fly down "Knockturn Alley" (Figure 2(a)) because it appeared in the analog orbiter image data to expose some of the best layered outcrop in steep cliffs but would otherwise be inaccessible to the rover. Such a flight might also allow the team to observe evidence of a fold or fault in the southern part of the ROI. The team was also interested in flying over the layered rocks of Unit 3 ("Forbidden Forest") and Unit 4 ("Azkaban") to better understand depositional and emplacement processes (Figure 2), and to aid in the selection of future rover exploration targets beyond the 5 sol duration of the simulation.

3.2. Simulated Mission Summary

A summary of the main activities planned and executed during Sols 101–105 and planned during Sols 106–110 is shown in Table 2. A detailed sol-by-sol account of the mission simulation can be found in the Appendix C, and a complete list of the activities planned for the rover and the helicopter can be found in Tables C1 and C2, respectively.

During Sols 101–105, the rover drove a total of 233 m over 4 sols, from the Sol 100 start point to Godric's Hollow (Figure 3(a)). The mission operations team opted to dedicate 1 sol (Sol 104) to proximity science and remote sensing at the "Specialis Revelio" outcrop (Figure 3(a) and Appendix C). The rover's stop at Specialis Revelio fulfilled the simulation

Table 2
Mission Sol Path

Mission Platform	Planning Cycle Sol	1 101	2 102	3 103	4 104	5 105	Look Ahead Plan 106	 107	 108	 109	 110
Rover	Location (Plan Start)	Sol 100 Starting Location	Spinners End	Specialis Revelio Workspace #1	Specialis Revelio Workspace #2	Specialis Revelio Workspace #2	Bloody Baron Workspace	Bloody Baron Workspace	Hogsmeade Penultimate	Hogsmeade Workspace	The Burrow
	Location (Plan End)	Spinners End	Grimmauld's Place (Specialis Revelio Workspace #1)	Specialis Revelio Workspace #2	Specialis Revelio Workspace #2	Godric's Hollow (Bloody Baron Workspace)	Bloody Baron Workspace	Hogsmeade Penultimate	Hogsmeade Workspace	Hogsmeade Workspace	The Burrow
	Main Activities	Pre-drive RS, 79 m drive (89.5 m actual) to Spinners End, reduced post-drive imaging (PDI) (180°)	Pre-drive RS, 60 m drive (59 m actual) to Grimmauld Place, mid-drive imaging, standard PDI, post-drive AEGIS	Pre-drive PS and RS, 2 m bump (1 m actual) to Grimmauld Place, standard PDI	RS, Abrasion, and PS	Pre-drive RS, 83 m drive to Godric's Hollow (Bloody Baron workspace), mid-drive imaging, reduced PDI (270)	RS, Abrasion, and PS	Pre-drive RS, 58 m drive to Hogsmeade, standard PDI	Pre-drive RS, Bump to Hogsmeade, standard PDI	RS, Abrasion, and PS	Pre-drive RS, TBD drive toward The Burrow, standard PDI
	Resource Limitation	Duration	Duration	Duration	Duration	Decisional Downlink	…	…	…	…	…
Helicopter	Location (Plan Start)	Sol 100 Starting Location	Flutterby Bush	Cleansweep	Chizpurfle	Bubotuber	…	…	…	…	…
	Location (Plan End)	Flutterby Bush	Cleansweep	Chizpurfle	Bubotuber	Bubotuber	…	…	…	…	…
	Main Activities	285 m flight over Spinners End and Grimmauld to landing site Flutterby Bush, high- and low-altitude surveys, imaging, VISIR	300 m flight over Knockturn Alley and Forbidden Forest to landing site Cleansweep, high- and low-altitude surveys, imaging, VISIR	294 m flight over Godric's Hollow and Hogsmeade to landing site Chizpurfle, high- and low-altitude surveys, imaging	147 m flight over Burrow to Bubotuber, low-altitude survey, imaging	297 m flight over Owlery and Azkaban returning to Bubotuber, low-altitude survey, imaging	TBD Heli flight skirting the Burrow; oblique images over potential rover outcrops	TBD Heli flight and imaging into The Burrow	TBD Heli Flight and imaging into The Burrow	TBD Heli Flight and imaging of Azkaban	TBD Heli flight toward next new ROI
	Resource Limitation	Distance constraint/landing site	Distance constraint/landing site	Energy; distance/landing site	None; science preference	Distance constraint/landing site	…	…	…	…	…

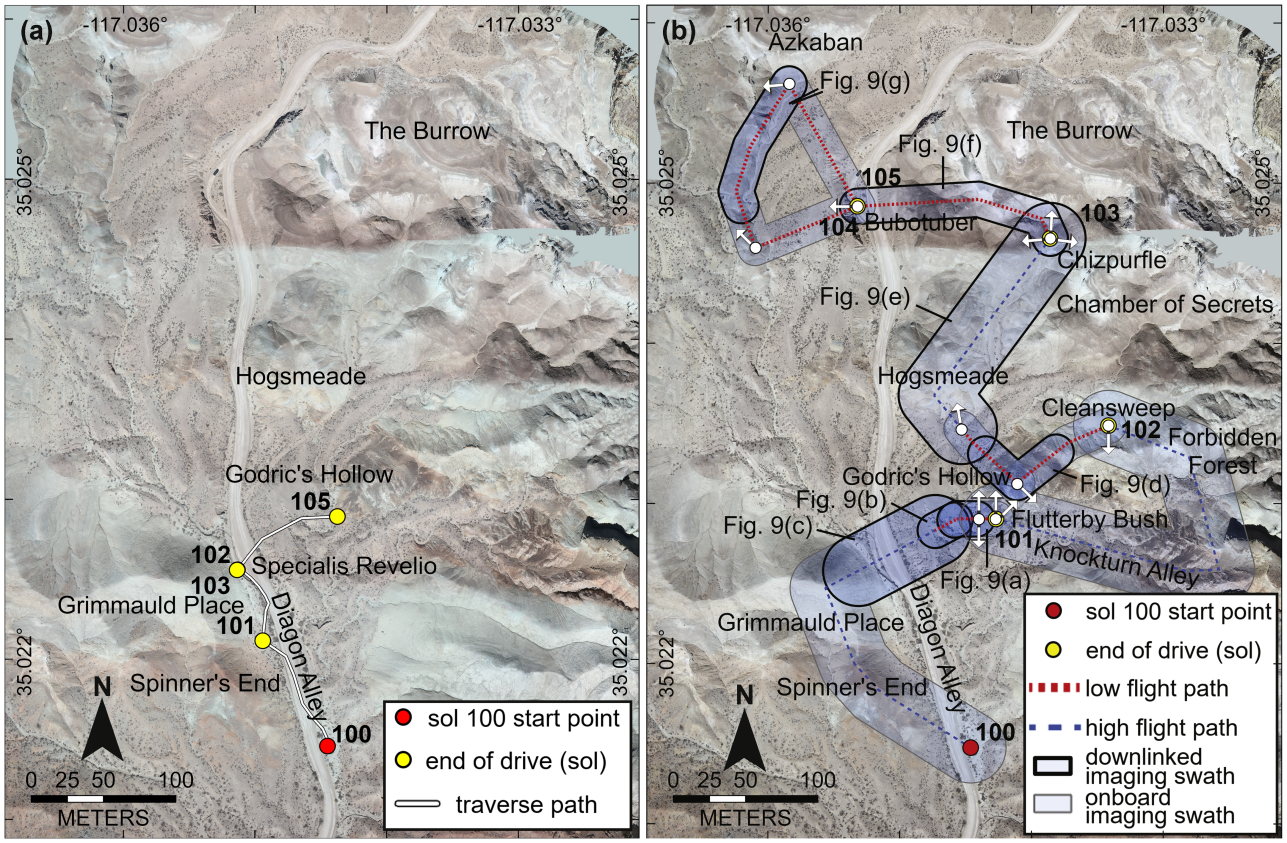

Figure 3. Rover traverse and helicopter flight maps. Maps showing the missions carried out by (a) the rover and (b) helicopter during the simulated joint rover-helicopter mission. White arrows show the viewing orientation of oblique images acquired by the helicopter. Image basemap: 2018 UAS orthomosaic.

constraint to deploy the rover's full science payload at least once, although this site was not that originally selected for proximity science during strategic planning (i.e., Godric's Hollow). The average distance traversed by the rover on its four mobility sols was 58 m, or 77 m over 3 sols if excluding the very short 2 m bump executed by the rover on Sol 103. During the 5 sol mission, the rover acquired seven independent Mastcam mosaic or image observations, took eight remote micro-imager (RMI) images or mosaics, and acquired four visible to near-infrared (VISIR) observations, three laser-induced breakdown spectroscopy (LIBS) observations, and three AEGIS targets including LIBS, VISIR, and RMI (Appendix C). Proximity science executed by the rover at one site (Specialis Revelio) included three X-ray flourescence (XRF) measurements, three Turretcam imaging suites, and two Raman measurements (Appendix C). During the mission simulation, the rover stayed in the southern half of the exploration area and was largely confined to exploring the route along Diagon Alley (Figure 3(b)). Four of the mission's sols (Sols 101–104) were duration limited (i.e., at or just below the plan duration constraint; Appendix C). The Sol 105 plan came in slightly under both energy and duration constraints because the team decided not to plan lower-priority activities with the remaining time or energy remaining (Appendix C).

As decided during the team's strategic planning process, the helicopter's first flight covered the entirety of the rover's likely traverse path during the simulation, landing in the vicinity of Godric's Hollow (Figure 3(b)). From there, the team commanded the helicopter to fly over terrain otherwise inaccessible to the rover (i.e., Knockturn Alley and Forbidden Forest; Figure 3(b)). The next series of flights took the rover to areas in the northern half of the ROI (e.g., "Hogsmeade," "The Burrow," and Azkaban) covering new geologic units and scouting potential future outcrops accessible to the rover (Figure 3(b)). The helicopter flew a total distance of 1322 m during the 5 sol mission, 707 of those meters in high-altitude survey imaging mode and 616 m in low-altitude survey imaging mode (Figure 3(b)). The helicopter acquired 13 low-altitude oblique images, acquired landed nadir images at three different landing sites, and collected two VISIR observations (Appendix C). None of the helicopter plans were duration or energy limited, but flights in four of the five plans (Sols 101–103, 105) were at or just under the simulation's 300 m flight distance constraint.

On the last day of the mission simulation, the team developed a plan for Sols 106–110, but with the expectation that this plan would not be executed by the field team in the context of the simulation (Table 2). The team anticipated that the rover would spend the next few days executing additional abrasion and proximity science, followed by drives north to explore the rest of the ROI. The team planned for the helicopter to fly north toward The Burrow, acquiring oblique images of potential outcrops accessible to the rover. The helicopter would then fly into The Burrow for further exploration of areas not necessarily accessible by the rover, before heading north to Azkaban and a new, yet-to-be determined ROI.

3.3. Data Downlink

During the 5 sol simulation, the mission operations team planned the acquisition of over 16 Gbits of science data with

the helicopter, which was about 2.5 times the amount of science data acquired by the rover (∼7 Gbits; Appendix D). Although the helicopter acquired significantly more total science data during the exercise, only 552 Mbits of helicopter data were designated as decisional and downlinked during the main simulation, compared with ∼1600 Mbits of rover data designated decisional (Table D1). During the first 2 sols of the simulation, minimal rover data were downlinked since the team prioritized downlinking the Godric's Hollow low-altitude survey and oblique images to enable enhanced rover localization and selection of a proximity science site. By Sol 103, which also coincided with the rover's arrival at Specialis Revelio, the team began prioritizing rover data for downlink because the remote-sensing data were decisional for proximity science targeting decisions. No helicopter science data were brought down in the decisional downlink on Sols 102–104. This was because the team recognized that data from terrain further afield were not needed to inform the subsequent day's plan for either the rover, which was exploring a different part of the field area, or the helicopter, which continued to carry out its reconnaissance survey over new terrain within the field area.

The team decided to bring down all remaining onboard rover data as part of the end-of-simulation large downlink pass on Sol 105 but decided to leave ∼8 Gbits of helicopter data on board indefinitely at the conclusion of the exercise (Appendix D). The data left on board included the Knockturn Alley high-altitude survey, which was of great scientific interest, but was not deemed necessary for near-term or future mission decisions. The team also decided to leave on board most of the low-altitude surveys from Sols 103 and 105, delaying this downlink until its value and impact to future rover traverse decisions was clearer.

4. Mission Science Observations

During the simulation, the mission operations team performed only the minimum analysis of science data needed to inform decisions about the upcoming sol's activities. This was analogous to real Mars missions, during which in-depth science analysis and interpretation often occurs on a strategic, rather than tactical or near-term timeline (e.g., S. M. Milkovich et al. 2022). The science observations collected by the rover and helicopter during this simulation are summarized below, primarily as an illustration of the type, content, and first-order science value of data sets collected by the respective mission platforms. In-depth scientific interpretation of these data sets was not considered in scope for this effort.

4.1. Rover

4.1.1. Imaging

Remote-sensing imaging observations acquired by the rover included Navcam, Mastcam, and RMI data from four sites: the Sol 100 starting point, Diagon Alley near the transition from "Spinners End" to "Grimmauld Place" (Sols 101–102), the Specialis Revelio workspace (Sols 102–105), and the "Bloody Baron" workspace at Godric's Hollow (Sol 105 end of drive) (Figure 3(a)). Context imaging revealed a rolling landscape strewn with a poorly sorted mix of sediments ranging from mud- to sand-sized to cobbles and boulders of variable color, rounding, angularity, and sedimentary and igneous lithologies, with occasional lightly cemented fluvial sediments (Figure 4). The slopes of prominent hills in the southern part of the exploration area (e.g., Spinners End and Grimmauld Place) were poorly consolidated with only rare, exposed bedrock (Figures 4(f) and (g)) and irregularly exposed patches of a bright white deposit on the lower slopes, sometimes hinting at structure within the slope (Figure 4(f)). Imaging of the Specialis Revelio outcrop provided a view of the alternating green and tan, fine-grained laminated bedrock (Figure 5(a)). In addition to discontinuous, parallel, wavy laminations comprising most of the Specialis Revelio outcrop, bulbous, centimeter- to decimeter-scale nodules were observed to be interbedded with the laminae (Figure 5(a)).

The team acquired rover Turretcam image suites for three targets at the Specialis Revelio workspace: "Fizzing Whizbees," "Twilfitt and Tatting," and "Bludger" (Figure 5). Turretcam images of Bludger revealed the brownish-white color variation within the nodule, as well as fine-scale evidence for the deformation of laminae around the nodule (Figure 5(b)), consistent with displacive formation before the surrounding layers had lithified. Turretcam images of the representative bedrock target Fizzing Whizbees confirmed the presence of subtle laminations and the very fine grain size of the rock as the few resolvable embedded grains appeared to be silt to very fine sand-sized (Figure 5(c)).

4.1.2. Composition

Six LIBS observations were acquired during the simulated rover mission, including AEGIS observations on Sols 100, 102 (a white knobbly layer later named Twilfitt and Tattings), 103 (Bludger nodule and "Venomous Tentacula" green layered bedrock), and Sol 104 ("Beauxbatons" red layered bedrock; Appendices C and E). Three XRF targets, Twilfitt and Tattings, Fizzing Whizbees, and Bludger (Figure 6 and Appendix E), were also acquired. All LIBS targets except the Sol 100 AEGIS, as well as all three XRF targets were acquired at the Specialis Revelio workspace. The Al_2O_3—CaO+Na_2O—K_2O (A—CN—K) ternary diagrams and element plots in Figure 6 show the compositional spread of the rover's LIBS and XRF measurements. The Twilfitt and Tattings target stands apart from the other four Specialis Revelio LIBS targets with a higher CaO composition, while the Sol 100 AEGIS observation on a suspected coarse crystalline igneous rock shows a trend toward higher K_2O and FeO in the A-CN-K and A-CNK-FM ternary diagrams compared to the other LIBS targets (Figures 6(a) and (b)). Bludger and Twilfitt and Tattings, the two nodular XRF targets, plot in the "CN" region of the A-CN-K ternary diagram shown in Figure 6. These targets show no Na in the XRF data, so their position on the ternary appears entirely dictated by Ca content, consistent with origins as secondary, diagenetic carbonate or carbonate-cemented nodules. In contrast, Fizzing Whizbees, the bedrock XRF target, plots near the apex of the A-CN-K ternary in the region consistent with high-aluminum clay minerals (Figure 6(a)). It is notable that the XRF data show a wider spread of compositions than those observed for corresponding targets in the LIBS data set (Figure 6). This discrepancy is not atypical of findings on Mars rovers, where the uncertainty associated with LIBS measurements is higher than that of complementary geochemistry instruments (e.g., A. H. Treiman et al. 2020).

The rover collected seven VISIR observations: two at the Sol 100 starting point (Sol 100 AEGIS and Sol 101 Hippogriff

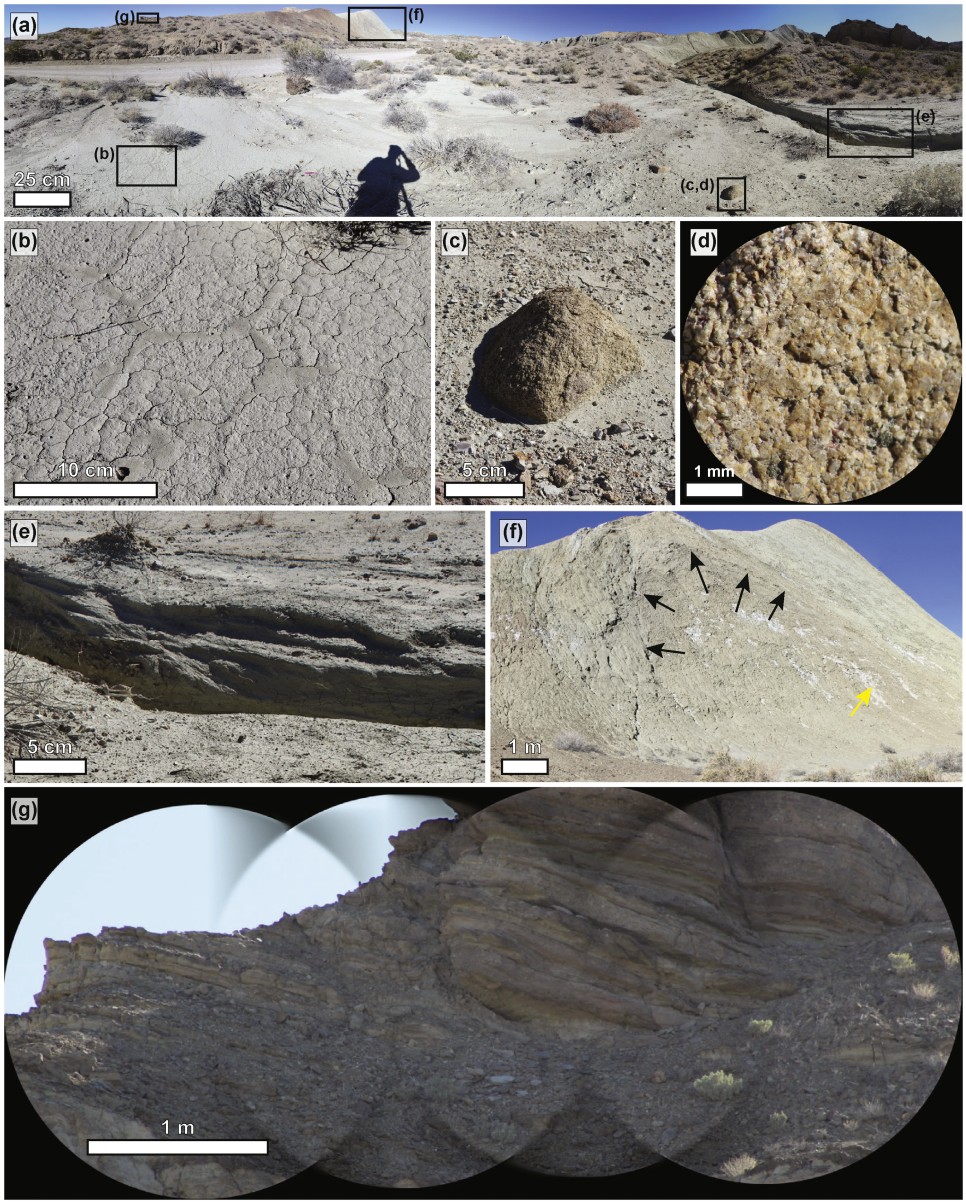

Figure 4. Landscape and outcrop images from the Sol 100–101 positions. (a) Sol 100 Navcam showing the landscape in the vicinity of the simulation starting position. (b) "Hippogriff" mudcrack target imaged on Sol 101. (c) Coarsely crystalline igneous cobble (Sol 100 AEGIS target) in the Sol 100 starting point workspace. (d) RMI image of the Sol 100 AEGIS target. (e) Sandy-pebbly bedforms exposed in a small cliff in the Navcam mosaic of the Sol 100 starting point. (f) Potential anticlinal fold structure (black arrows) observed in the Sol 101 Navcam on the slope of Grimmauld Place. (g) Resistant layered caprock of the "Durmstrang" target acquired on Sol 101.

targets), one along Diagon Alley at the base of the Spinners End slope (Sol 102 Lumos target), and four at the Specialis Revelio workspace (Twilfitt and Tattings, Sol 103 AEGIS, Venomous Tentacula, and Bludger targets) (Figure 7 and Appendix C). The spectra of targets acquired on Sols 100–102 (prior to Specialis Revelio) are dominated by smectite absorptions near ∼1400 nm, ∼1900 nm, and 2250–2350 nm (Figure 7(a)). Absorptions short of 1000 nm (particularly 925 nm) suggest Fe-bearing minerals, such as a ferric iron silicate, oxide, or hydroxide. Absorptions in the shortwave half of the spectrum may be indicative of chlorite and/or goethite (Figure 7(a)). The rover's VISIR observations of bedrock targets acquired at Specialis Revelio are consistent with montmorillonite, goethite, and some carbonate (Figure 7(a)). The Bludger nodule target shows the most distinct spectra compared to the other targets, with absorptions suggestive of hectorite mixed with carbonate. Rover RMI observations together with the VISIR-derived mineralogy are consistent with Bludger being a clay- and carbonate-bearing nodule (Figures 5(b) and 7(a)).

Raman data were acquired on two targets at the Specialis Revelio workspace, the Bludger nodule and the Fizzing Whizbees green layered bedrock target. Carbonate appears to be present in the Raman spectra of Bludger with a peak at $\sim$1100 cm^{-1}, but the fluorescence of the spectra is too high to resolve *G*- or *D*-band organic signals (Figure 8(a)). The Fizzing Whizbees spectrum looks similar to that of montmorillonite, possibly mixed with other phyllosilicate minerals, generally consistent with the XRF and LIBS results (Figure 8(b)). The broad feature at $\sim$1000 cm^{-1} present in both samples may represent an amorphous component, while the features at higher wavenumbers (>2000 cm^{-1}) could be

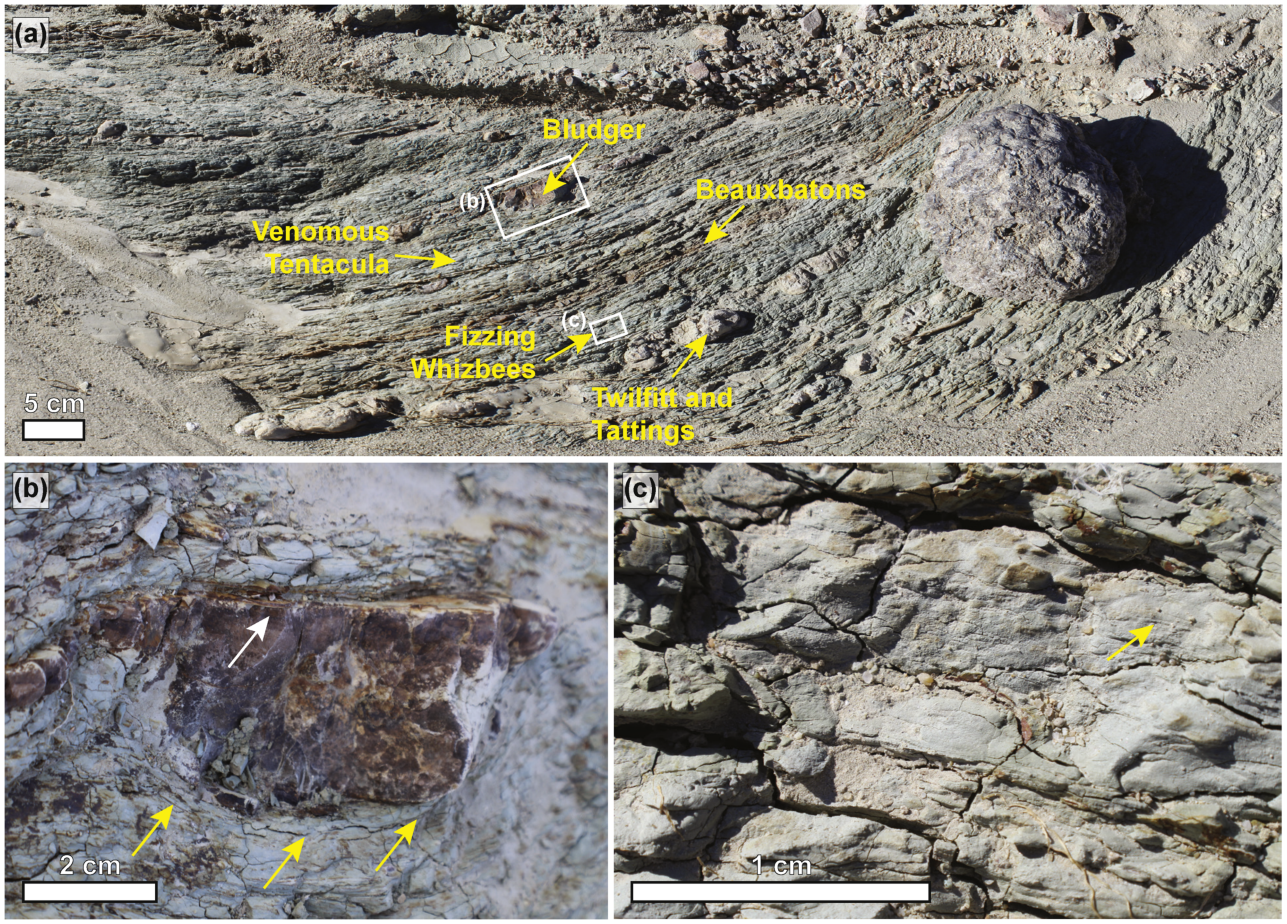

Figure 5. The Specialis Revelio Workspace. (a) Sol 102 Navcam view of the Specialis Revelio workspace. (b) Turretcam image of the Bludger nodule acquired on Sol 104. Yellow arrows point to deformed laminations around the base of the nodule, white arrow points to lamination in the upper part of the nodule. (c) Fizzing Whizbees target imaged by Turretcam on Sol 103. Yellow arrow points to subtle thin laminations within the outcrop.

due to the presence of hydration, or the second-order peaks of other minerals.

4.2. Helicopter

4.2.1. Imaging Surveys

The only helicopter image survey designated as decisional data during the mission simulation was a portion of the low-altitude survey acquired on Sol 101 that covered ∼30 m of the rover's planned approach to Godric's Hollow to scout out an outcrop for the rover's proximity science investigation and to enable the rover's enhanced localization at this site (Figures 9(a) and (b), Appendix D). The survey imaged relatively flat-lying terrain composed predominantly of unconsolidated sediment. A gully cutting through the steep slope that forms the western edge of Godric's Hollow slope revealed the only possible bedrock cropping out within the scene (Figure 10(b)).

As part of the large downlink pass at the end of the simulation, the team requested a portion of the Sol 101 high-altitude survey that covered the Specialis Revelio workspace for additional geologic context for rover observations (Figures 9(c) and 10(a)). The western portion of the mosaic covers the steep, gray-green slope of Grimmauld Place with several small terraces and some decimeter-scale clasts resolvable at the base of the hill (Figure 10(a)). The Specialis Revelio outcrop was not identified in either the helicopter image or the orbiter data, in large part because the source data for both data sets were acquired several years prior to the mission simulation and because the image was altered to remove evidence of a human-made road (Figure 10(a)).

The team downlinked additional segments of the Sol 103–105 low- and high-altitude surveys covering Godric's Hollow, Hogsmeade, Chizpurfle, The Burrow, and Azkaban (Figures 9(d)–(g)). Compared to the orbiter data, the helicopter mosaics sometimes enabled the resolution of additional layers and finer-scale structure (e.g., Godric's Hollow; Figure 10(c)). Well-preserved bedrock is generally rare, as the terrain comprises recessively weathering slopes of textural uniformity (e.g., Hogsmeade; Figure 9(e)), although the paucity of resolvable cobbles and boulders suggests that the bedrock forming these slopes is likely relatively fine-grained. Resistant and light-toned bedrock ridges are resolvable in the Sol 104 low-altitude survey covering the southern extent of The Burrow (Figure 9(f)) and Azkaban (Figure 9(g)). The hills exposed in the southernmost portion of the survey show a distinctly different, steeper dip compared to the hills to the north, suggesting the presence of a fault in this area (Figure 9(g)). The observation of alternating relatively thin layers is more consistent with an aqueous depositional environment involving episodic sedimentation than an igneous origin, such as pyroclastic deposition, and would be a high priority for future rover exploration.

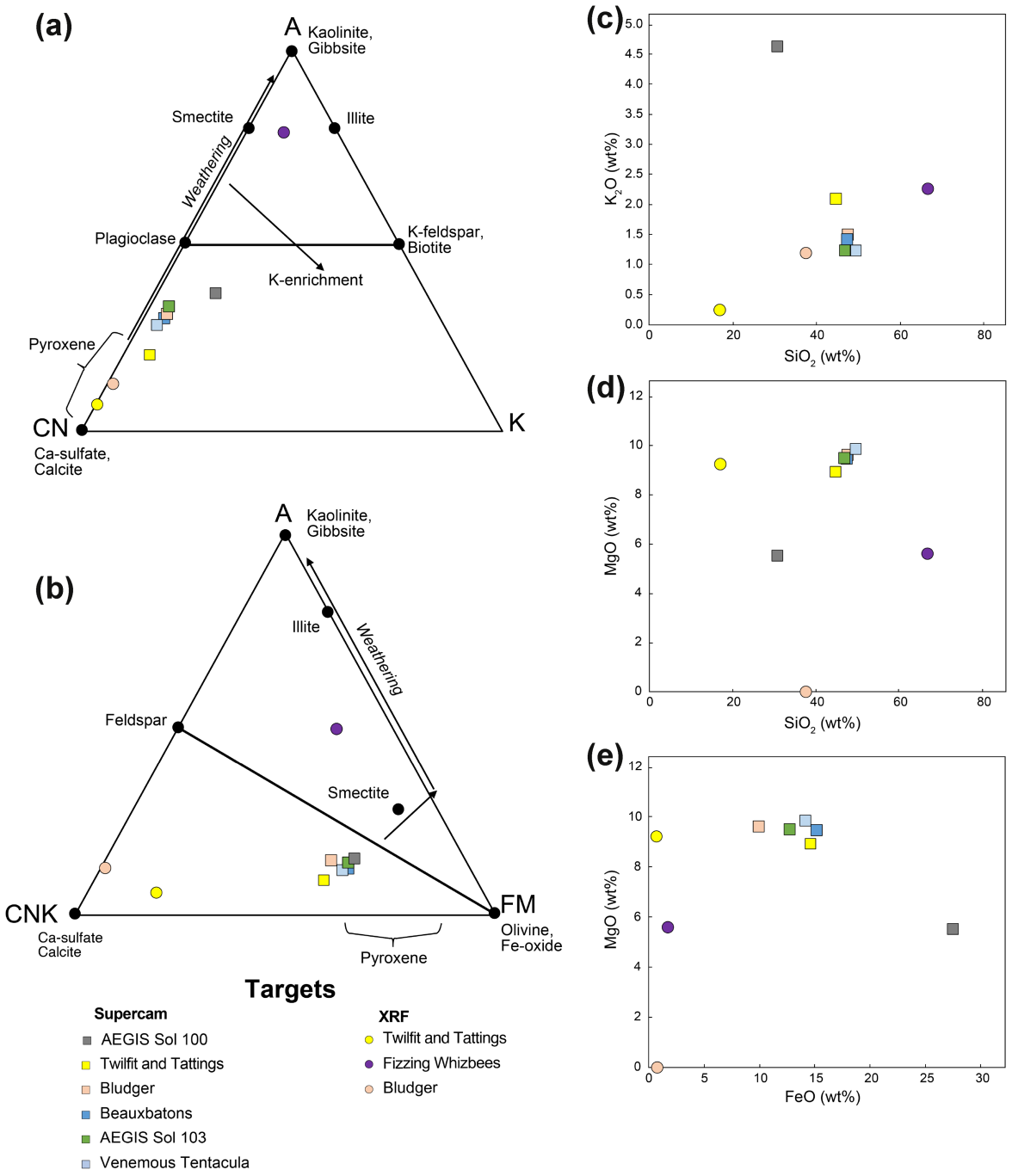

Figure 6. Major element compositions for the rover's LIBS and XRF targets. (a) A-CN-K diagram. (b) A-CNK-FM diagram. (c) Plot of K_2O vs. SiO_2. (d) Plot of MgO vs. SiO_2. (e) Plot of FeO vs. MgO.

4.2.2. Oblique Images

Low-altitude oblique images were taken during each of the helicopter's five flights, commonly during landing, and sometimes during dedicated mid-flight locations when the helicopter was traversing a particularly interesting area identified in advance in the orbiter image data set (Figure 11). The Sol 101 oblique images provide a view of two locations at Godric's Hollow that were under consideration for the rover's proximity science (Figures 11(a) and (b)). These images provided early insight into the location and limited extent of potential bedrock for proximity science at this site. These images also enabled the resolution of sand- to boulder-sized clasts in the dry streambeds at the base of Godric's Hollow (Figures 11(a) and (b)).

The Sol 102–105 oblique helicopter images document bedrock stratigraphy, including variations in color, layer thickness, weathering properties, and structural orientation, or, in some cases, the absence of bedrock (Figure 11). The Sol 102 oblique helicopter image gave an upslope view at the Cleansweep landing site (Figure 11(c)), revealing that the majority of the slope was covered in a fine-grained crust (Figure 11(c)). The Sol 103 oblique images of Godric's Hollow and Hogsmeade were more successful at imaging bedrock (Figures 11(d) and (e)), and the oblique image acquired on Sol 104 near Bubotuber shows a sequence of

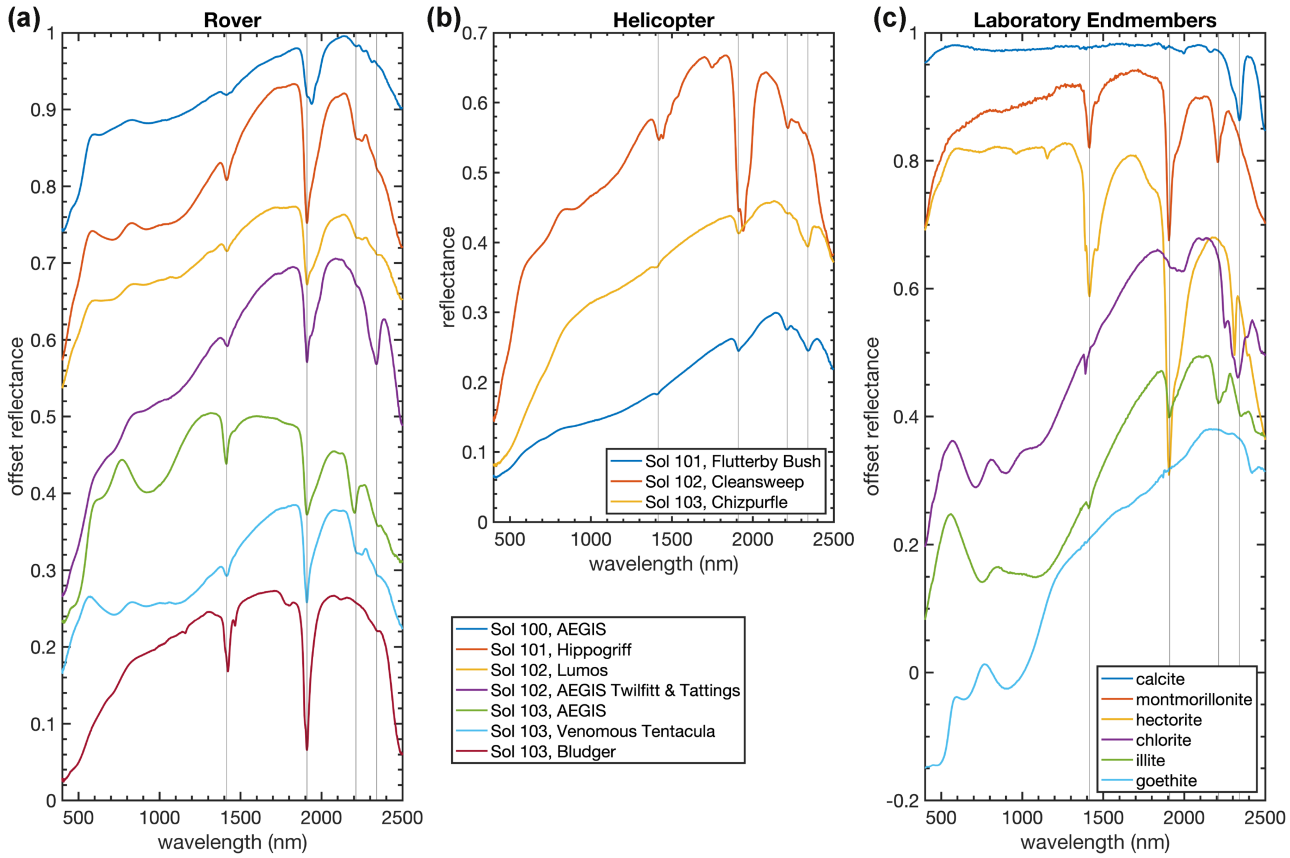

Figure 7. Visible to near-infrared (VISIR) reflectance spectra collected during the simulation. (a) VISIR spectra collected by the rover. The spectra displayed (and their vertical offsets in parentheses) include Sol 100 AEGIS (+0.65), Sol 101 Hippogriff (+0.4), Sol 102, "Lumos" (+0.3), Sol 102 AEGIS Twilfitt and Tattings (+0.1), Sol 103 AEGIS (+0.1), Sol 103, Venomous Tentacula (+0.05), and Sol 103 Bludger (−0.05). (b) VISIR spectra collected by the helicopter. The spectra displayed (with no vertical offsets) include Sol 101 "Flutterby Bush," Sol 102 "Cleansweep," and Sol 103 "Chizpurfle." (c) Laboratory reference spectra from NASA's Reflectance Laboratory. Spectra displayed are calcite (CACA10), montmorillonite, (CAMO02), hectorite (C1EA27A), chlorite (C1EA14), illite (C1JB782A), and goethite (CAHO03). All reference spectra are of <45 μm particle size. All three subplots have reference lines at 1415, 1910, 2212, and 2340 nm.

apparently north-dipping greenish beds of variable thickness (Figure 11(f)). The oblique image of Owlery shows a rough, gray slope whose crusty surface is covered by coarse sediment estimated to be granule and pebble size (Figure 11(g)). The northward-looking oblique image of Azkaban shows a similar pebbly crust covering most of the low-relief, nearfield of the image, but distinct east-dipping tan, brown, and green layers can be observed in the steeper slopes of the background (Figure 11(h)).

4.2.3. Landed Observations

The nadir landed helicopter images acquired at Flutterby Bush (Sol 101), Chizpurfle (Sol 103), and Bubotuber (Sol 104) and downlinked at the end of the exercise show an assortment of distinct clast populations of variable color, size, sorting, and angularity that appear representative of variations in local bedrock sources (Figure 12). The Sol 102 landed image acquired at Cleansweep shows a very different surface composed predominantly of a light gray/tan, very fine-grained unit with a chunky cauliflower-like surface texture (Figure 12(b)). Small, tan/brown clasts that are highly angular appear partially embedded within the fine-grained gray unit (Figure 12(b)).

Three VISIR measurements were acquired by the helicopter at Flutterby Bush (Sol 101), Cleansweep (Sol 102), and Chizpurfle (Sol 103) (Figure 7(b)). Flutterby Bush and Chizpurfle exhibit absorption features consistent with a mixture of smectite (likely montmorillonite) and carbonate (Figure 7(b)). The Sol 102 Cleansweep spectrum exhibits absorption features consistent with montmorillonite and illite/chlorite (Figure 7(b)), but absorptions suggestive of sulfate (Figure 7(c)), namely gypsum, make it a unique mineral identification in the VISIR suite. The helicopter VISIR measurements tend to include shallower absorption features than the rover's measurements, and the rover spectra show a greater variety of mineral absorption features and interpreted mineralogy (Figure 7).

5. Discussion

5.1. Advantages and Limitations of the Simulated Mission Platforms

This dual-platform simulation provided an opportunity to observe the strengths and challenges associated with the rover and helicopter individually and in tandem as a combined mission architecture.

5.1.1. Rover

Science data acquired during the mission simulation demonstrated well the rover's ability to collect nested contextual images and compositional analyses from landscape to microscales. These results are consistent with previous rover

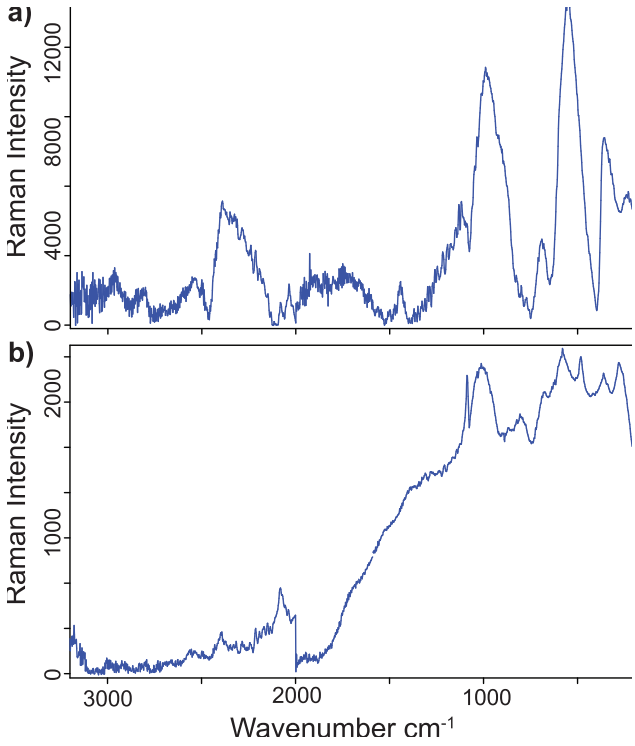

Figure 8. Raman spectra of the Bludger and Fizzing Whizbees targets. (a) Raman spectrum from the Bludger nodule target acquired on Sol 104. (b) Raman spectrum of the Fizzing Whizbees bedrock target acquired on Sol 104.

analog studies (e.g., R. A. Yingst et al. 2016, 2020, 2022; G. R. Osinski et al. 2019; S. Gwizd et al. 2024) as well as a body of literature built over nearly three decades reporting results from rovers on the surface of Mars. On a relatively rapid sol-by-sol turnaround time, contextual data were used to target increasingly resource intensive and complex payload investigations (i.e., proximity science), allowing the team to prioritize the most compelling science targets for detailed analysis at the finest scales. The rover's investigation at Specialis Revelio served as the best example of this cadence. When the Sol 102 post-drive Navcam Panorama and Mastcam workspace mosaic image data sets revealed the presence of a compelling outcrop, the team was able to respond and pivot quickly to remain at the outcrop. The team used these contextual image data sets to plan follow-up remote-sensing observations on the Bludger nodule target on Sol 103. The LIBS, RMI, and VISIR data of Bludger, which showed carbonate and clay signatures, were then used to motivate follow-up Turretcam, XRF, and Raman observations on Sol 104 once it was deemed to be one of the most compelling targets within the workspace. These detailed observations confirmed the composition of the Bludger nodule and yielded important constraints on the early diagenetic timing of nodule formation due to the presence of deformed laminae around the nodule (Figure 4(b)). The rover also acquired a mix of long-distance observations (e.g., the long-distance RMI and mosaics of the surrounding hills at Spinners End and Grimmauld Place), and near- and midfield outcrop observations like the Hippogriff mudcracks, fluvial outcrops imaged mid-drive, and the surrounding Specialis Revelio bedrock which could be used to place depositional and stratigraphic constraints on the bedrock geology observed in the ROI (Figures 4 and 5).

The simulated mission's science return was also enhanced by the rover's ability to accommodate a multi-instrument science payload. In addition to its four cameras (Navcam, Mastcam, RMI, and Turretcam), the rover carried two instruments on the mast and two on the turret to interrogate bulk geochemistry and mineralogy. This payload allowed mineralogical and geochemical analysis on nearly every sol of the mission, as well as coordinated remote-sensing and proximity science observations on several targets in the Specialis Revelio workspace. The Bludger target again shows the value of these coordinated observations. LIBS, VISIR, XRF, and Raman all gave some indication that carbonate was present in the nodule—thereby increasing the team's confidence in this interpretation—but VISIR also revealed the presence of a strong clay signature in the nodule, not otherwise observed by the other techniques (e.g., Figure 7(a)). Overlapping instrument capabilities also presented challenges in reconciling discrepancies between the data sets, particularly on the rapid tactical timeline. In Figure 6, the geochemical plots show that XRF and LIBS data from the same Twilfitt and Tattings target show significant variability in composition when plotted on ternary diagrams. Such discrepancies have been observed with similar payloads on real rover missions (e.g., A. H. Treiman et al. 2020), perhaps due to the differing spot size of the instruments, but satisfactory explanations for these discrepancies are not always found.

The simulation also illustrated the rover's traversability limitations. With the ability to traverse only $\sim$100 m sol^{-1}, the rover was limited to exploring only the southern half of the ROI during the 5 sol mission. It is worth noting that the Perseverance rover's autonavigation capabilities allow it to achieve up to 200–300 m in a single sol if the terrain is benign, and autonomous driving is an area of active research (e.g., R. M. Swan et al. 2021). The impact of drive constraints will be lessened for some current and future rover missions. However, even with the possibility of longer traverses, rovers are still limited to driving over relatively benign, low-slope terrain. Yet in this field area, as is likely the case on Mars, many of the most interesting outcrops are exposed at higher slopes and in steep cliff faces that were ruled out-of-bounds for the rover for safety reasons. This simulation's rover felt this impact most strongly along its traverse through Diagon Alley. Since outcrop turned out to be relatively rare within the southern part of the field area at locations accessible to the rover, the utility of the rover's sophisticated payload was limited not just by the duration of the mission simulation, but also the accessible bedrock outcrop.

5.1.2. Helicopter

The helicopter showed its versatility and mobility in the extensive survey of the terrain it carried out across the exploration region during the mission simulation. The helicopter covered more than 5 times the distance traversed by the rover, capturing either high- or low-altitude surveys over its entire flight path. While the rover was limited to the southern portion of the ROI, the helicopter covered the rover's entire 5 sol traverse in a single sol, then proceeded on to terrains either inaccessible to the rover because of safety constraints or candidate future exploration sites for the rover beyond the limited duration of the simulation. In particular, the helicopter was able to head east over Knockturn Alley and Forbidden Forest, areas inaccessible to the rover (Figures B1 and 3(b)), and to the north, collecting image data over The Burrow and Azkaban.

Figure 9. Helicopter imaging surveys downlinked during the simulation. (a) Low-altitude (10 m above ground level) survey covering the approach to Godric's Hollow acquired by the helicopter on Sol 101. (b) Low-altitude survey acquired on Sol 101 covering the candidate proximity science stop at Godric's Hollow. (c) High-altitude (20 m above ground level) survey acquired on Sol 101 covering the Specialis Revelio workspace and the slope of Grimmauld Place. (d) Low-altitude survey acquired on Sol 103 of Godric's Hollow. (e) High-altitude survey acquired on Sol 103 covering Hogsmeade to Chizpurfle. Note the color artifact at the northern end of the survey. (f) Sol 104 low-altitude survey from Chizpurfle to "Bubotuber." Note the color artifact at the eastern end of the survey. (g) Low-altitude survey acquired on Sol 105 from "Owlery" (south) to Azkaban (north). Survey flight swaths have been localized on Figure 3(b).

Both the low- and high-altitude surveys, at 3 and 6 cm pixel^{-1} resolutions, respectively, provided substantial improvements over the HiRISE-equivalent 25 cm pixel^{-1} orbiter data. From the orbiter image data, it was possible for the team to resolve color and meter-scale textural variations in resistance to weathering of the major units (Figure 2). Based on the orbiter image data and the color similarities of exposures throughout the ROI, the team favored an interpretation of a fold in the southern region to explain the repetition of red (Unit 1) and white (Unit 2) units. However, after imaging these exposures with the helicopter, it became clear that the red bedrock of Unit 1 represented at least two distinct units. The southern red bedrock exposure appears to be well consolidated and cliff-forming with distinct layering, and was likely not a repetition of the same unit to the north, where the reddish color originated from eroding reddish layers interbedded with lighter yellow layers (Figure 9).

Analog orbiter image data enabled the identification of several meter- to decameter-scale layering within the best-preserved outcrops of the ROI (e.g., Knockturn Alley, Godric's Hollow), and there appeared to be several identifiable beds that could be followed for short distances. Though it was unclear how these

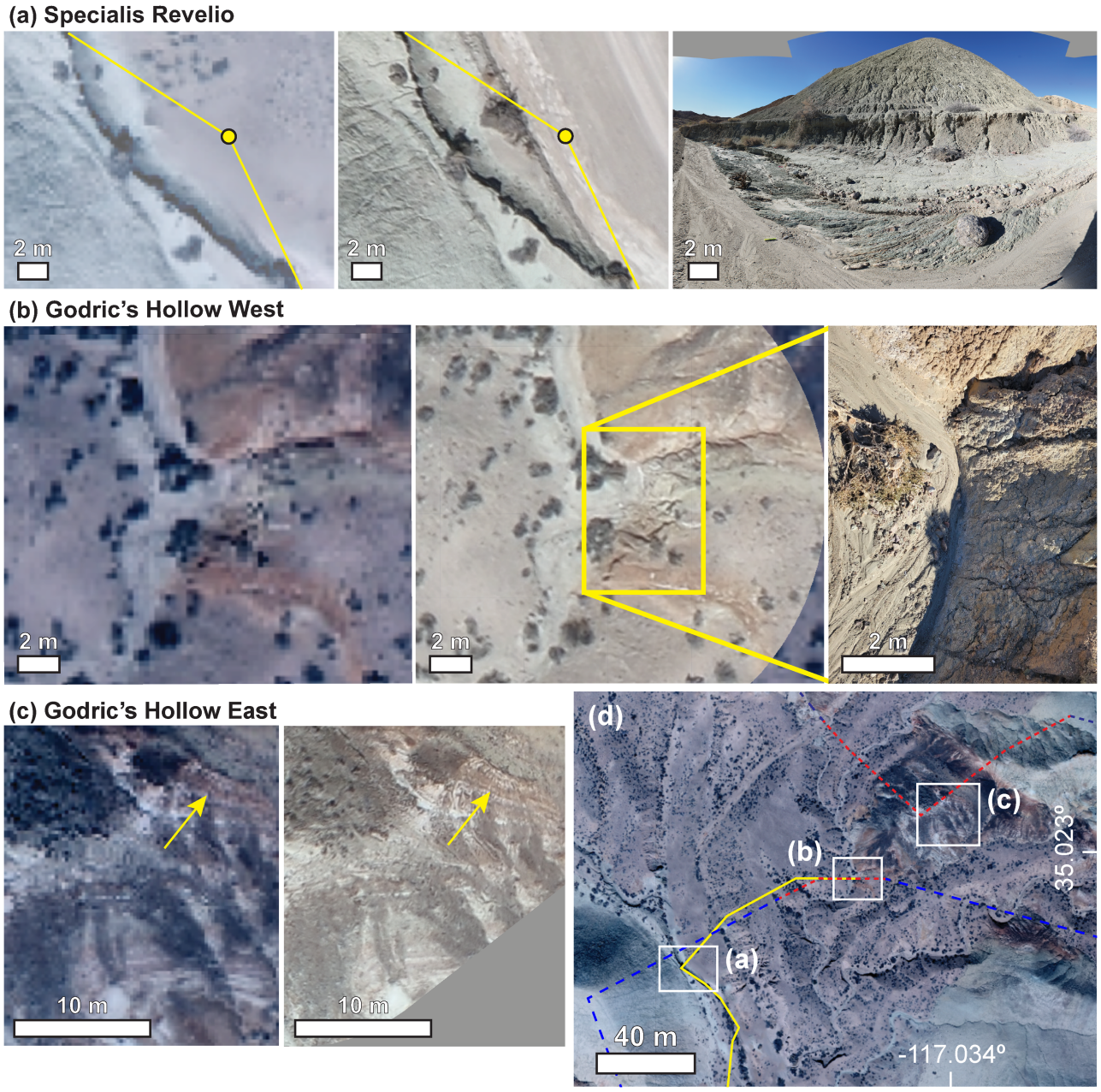

Figure 10. Comparison between orbiter, helicopter survey and oblique images, and rover view. (a) Specialis Revelio workspace observed, from left to right, at the scale of orbiter HiRISE, high-altitude helicopter survey, and rover Navcam. The yellow dot shows the location of the rover from which the rover Navcam (far-right panel) was taken, and the yellow lines show an approximation of the FOV of the Navcam mosaic. (b) Western slope of Godric's Hollow observed, from left to right, at the scale of orbiter HiRISE, low-altitude helicopter survey, oblique helicopter image. (c) Eastern slope of Godric's Hollow observed, from left to right, at the scale of orbiter HiRISE and low-altitude helicopter. (d) Locator map for sites (a) through (c) showing a portion of the rover and helicopter's traverse and flight paths, respectively. The yellow line represents the rover traverse, the blue dashed line represents high-altitude helicopter survey paths, and the red dashed line represents low-altitude helicopter survey paths.

layers connected, the team assumed that bedrock would be present on the ground. However, the high- and low-altitude helicopter survey images confirmed the paucity of bedrock outcrops in the ROI and the poor consolidation on the sloped surfaces of hills (Figure 9). Yet in the areas of the Specialis Revelio and Bloody Baron workspaces, the team struggled, even with these enhanced-resolution survey data sets, to identify good bedrock outcrops for the rover to visit (Figure 10). Rather, it was really the low-altitude oblique imaging that proved most useful for this purpose.

These low-altitude oblique images were particularly useful for assessing the quality and exposure of bedrock for potential future exploration by the rover, and it was these images of Godric's Hollow that the team used to select the Bloody Baron workspace as a future destination of the rover (Figures 11(a) and (b)). The oblique images also provided the best viewing perspective of outcrops from a science perspective. The oblique images allowed the team to resolve centimeter- to decimeter-scale stratigraphy and clasts exposed in vertical cliff faces as well as the structural orientation of bedding not otherwise observable in the HiRISE images, helicopter image surveys, or nadir landed images. In general, the nadir images were of limited science utility to the team for the purposes of understanding the bedrock geology of the field area since the low-slope, low-roughness constraints for helicopter landing

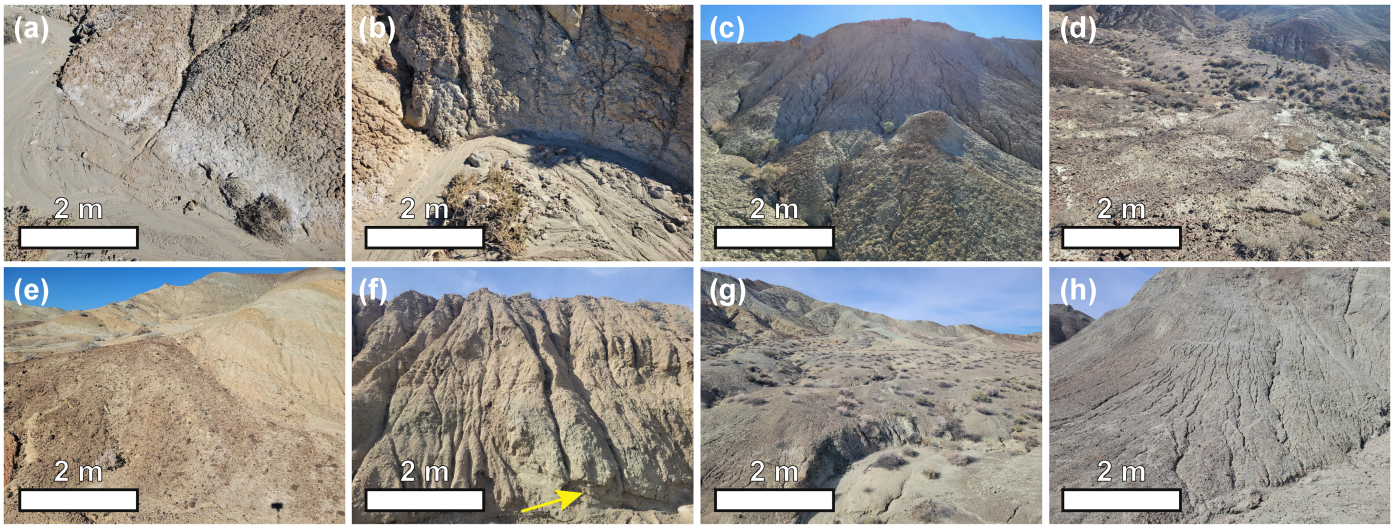

Figure 11. Low-elevation (5 m above ground level) oblique images acquired by the helicopter. (a) View to the north of the west-facing slope of Godric's Hollow acquired on Sol 101. (b) View to the south of the west-facing slope of Godric's Hollow acquired on Sol 101. (c) Slope south of the Chizpurfle landing site acquired on Sol 102. (d) View toward the southeast taken north of Godric's Hollow on Sol 103. (e) Base of Hogsmeade slope acquired on Sol 103. (f) View of east-facing scarp west of the Bubotuber landing site acquired on Sol 104; the yellow arrow points to a greenish, layered outcrop at the base of the scarp. (g) View to the northwest of Owlery acquired on Sol 105. (h) View to the west of Azkaban sequence acquired on Sol 105.

Figure 12. Images of the helicopter's landing sites acquired by the nadir-pointed camera. (a) Flutteryby Bush landing site imaged on Sol 101. (b) Cleansweep landing site imaged on Sol 102. (c) Chizpurfle landing site imaged on Sol 103. (d) Bubotuber landing site imaged on Sol 104.

sites meant that these images were usually taken on loose sand and pebbles rather than in-place bedrock outcrop. Such documentation is not without science value, though, as proven by analysis of clast surveys acquired by Spirit (R. A. Yingst et al. 2010) and Curiosity (e.g., R. A. Yingst et al. 2013, 2016; S. Y. Khan et al. 2022).

The helicopter benefited from increased mobility compared to the rover in this simulation, but it is still worth noting that the low-slope landing site constraint did limit the team's use of the helicopter to explore the highest-priority bedrock exposures, which were often in high-slope challenging terrains without nearby safe landing sites. This challenge was compounded by

the ∼300 m flight distance limitation imposed during this simulation, which was most often the limiting factor in planning helicopter flights. While it may be reasonable to assume that future helicopters on Mars would be able to exceed 300 m in single sol flights and take advantage of improved autonomous landing capabilities (J. Bapst et al. 2021), safe landing constraints are still likely to limit a helicopter's ability to explore certain high-slope, rough terrain.

The helicopter's limited science payload was an intentional choice in the design of this mission simulation, but it is realistic to assume that a helicopter's instrumentation and targeting ability would be limited compared to that standardized by recent large rovers on Mars (e.g., J. Bapst et al. 2021). The inclusion of the VISIR instrument on this simulation's helicopter did enable a characterization and comparison of the composition of different landing sites and provided data that could be compared with a similar data set acquired by the rover. However, the utility of the landed VISIR instrument was limited in a similar way as the nadir landed images (i.e., the inability to target, coupled with the helicopter's need to land on benign terrain meant that the VISIR data sampled mostly alluvium float deposits rather than bedrock). As a result, the helicopter's VISIR data set showed less spectral diversity than the rover's, even though the helicopter had the ability to explore new and different units throughout the ROI. A hyperspectral imaging spectrometer that could be coupled with the oblique images would likely have proven a more useful scientific instrument in the context of this mission scenario.

5.2. Science Value of a Joint Rover and Helicopter Mission

Both the rover and the helicopter have their advantages as individual mission platforms but together form a powerful and capable combination of breadth and depth. A rover provides a ground-based perspective on geologic context and the opportunity for progressively higher-resolution spatial analyses of rock targets. The ability of a rover to carry a larger payload provides an opportunity for complementary and coordinated observations with different analytical techniques. A helicopter enables exploration beyond that typically possible with a rover within a given amount of time, and in terrains inaccessible to rovers. While high- and low-altitude images surveys can provide a higher-resolution view of the landscape than that offered by orbiter images, oblique images provide the best opportunity for scouting outcrops for future rover exploration and for providing a view of outcrop stratigraphy.

Although a joint mission has clear science advantages over a single platform mission, a dual-platform architecture comes with increased development and operational costs. Such a mission architecture, which would almost certainly be considered flagship-class if it involved a Curiosity/Perseverance-type rover, is not currently being prioritized in the most recent decadal survey (National Academies of Sciences, Engineering, and Medicine 2023). However, mission architectures pairing a helicopter with a smaller, Mars Exploration Rover–class rover may be more tractable for future competed mission opportunities.

5.3. Value of Enhanced Rover Localization Using Helicopter Data

One of the operational capabilities this exercise sought to simulate was enhanced localization for the rover using helicopter image data. The team attempted to exercise this capability once the Godric's Hollow site had been identified during strategic planning as a likely site for proximity science investigation. On Sol 101, the team planned a low-altitude helicopter survey along the rover's likely approach route toward Godric's Hollow, anticipating that the rover would arrive there 2–3 sols into the exercise. The team requested the first ∼15 m of this survey as part of the decisional downlink planned on Sol 101, with the second ∼15 m of the survey requested as part of the decisional downlink planned on Sol 102. The team quickly realized that low-altitude helicopter survey segments consumed most of the daily decisional downlink budget and prevented the return of most science data during the first half of the simulation, including helicopter images over other parts of the rover's notional traverse. Thus, prioritizing the downlink of helicopter data to enable the rover's enhanced localization at Godric's Hollow limited the team's ability to use helicopter images to scout terrain prior to Godric's Hollow, since these data remained on board until the nondecisional downlink at the end of the simulation. Ultimately, the rover's fortuitous discovery of the Specialis Revelio outcrop superseded the team's original interest in the strategically selected Godric's Hollow site for proximity science. Although the team did decide to continue to Godric's Hollow for a brief stop in the Sol 106–110 Look Ahead Plan (or LAP) and anticipated saving a sol thanks to the enhanced localization capability, the general impression of the team was that the decisional data volume budget earlier in the exercise would have been better spent on downlinking other science data besides the low-altitude survey data at Godric's Hollow. The team thus experienced the cost of going "all-in" on a strategically identified outcrop from orbit (i.e., Godric's Hollow), which turned out to be less interesting to the team than Specialis Revelio. Given the steep downlink cost of executing enhanced localization when planned only several days in advance, the team decided not to use this capability again during the exercise.

For a capability like enhanced localization using helicopter data to be practical for a joint rover-helicopter mission, onboard processing of the helicopter data (e.g., R. Brockers et al. 2022), without requiring "ground-in-the-loop" processing by the Earth team, is likely needed to make this practical for use in a 1 to several sol near-term planning timescale demanded by a rover. Alternatively, a capability like that practiced in this simulation could be useful if the helicopter were to travel sufficiently out front of the rover such that ample time exists for the low-altitude survey data to be downlinked opportunistically without a negative impact on tactical or near-term decision-making for the rover or the helicopter.

5.4. Key Observations and Lessons Learned

The main objective of this exercise was to test and develop strategies for the joint operation of a combined rover and helicopter mission in a Mars analog setting. Although the team designed an operations process intended to give equal planning time and consideration to both the rover and the helicopter, the rover generally dominated tactical operations planning given the complexity and number of daily decisions that needed to be made about the rover's operation. The helicopter required science input during the discussion of a flight path, but with limited science observation options and low planning complexity of those options, decisions about the inclusion of oblique images or landed science were relatively straightforward. The

team found that the most efficient way to build the helicopter plan was to have the Helicopter Representative work independently to develop a proposed flight path and imaging plan. The Helicopter Representative would then present and discuss this plan with the full team. The helicopter's ability to acquire continuous mid-flight science observations, i.e., imaging surveys, and numerous mid-flight stops along the flight path, meant that science input was a primary driver for the design of the entire length of the flight path. In contrast, the rover's emphasis on end-of-drive targeted observations meant that science input often drove the selection of the rover's end position and rare mid-drive stops, but the majority of the rover's drive path was science-agnostic. Following agreement on the helicopter flight plan, the team worked together to determine helicopter downlink priorities since they were most often dependent on the decisional needs of the rover mission. As the exercise progressed and the helicopter flew further afield from the rover, the helicopter plan became less dependent on the tactical rover plan, and vice versa.

The mission operations team decided during the main exercise to bring down more than 3 times the amount of rover data decisionally than helicopter data. This related to the fact that data acquired by the rover on one sol often fed directly into the next sol's planning, and thus required a more "reactive" planning approach (L. Cheng et al. 2008; S. M. Milkovich et al. 2022). For example, remote-sensing science observations were needed to decide on proximity science targets, and both data sets were used to determine whether the rover would remain at its current workspace or plan a drive away. The helicopter, on the other hand, with its fewer science instruments, simplified operational modes, long flight distances, and large data volume image surveys, was limited in its ability and need to respond to data acquired on any given sol. Thus, the team deprioritized helicopter data for decisional downlink. Given the large data volume of helicopter imaging surveys, the team found that it was impractical to downlink much of this data on the timescale of the 5 sol simulation, and that much of these surveys was not needed for tactical or near-term rover planning with the rover, especially when the surveys covered terrain inaccessible to the rover. Rather, some carefully planned and specifically targeted oblique images at sites relevant to the rover's exploration were of greatest value from a near-term operations and science impact versus downlink cost perspective, with the team satisfied to leave most of the longer and higher-data-volume surveys on board to come down opportunistically later. The data volume challenges observed in this simulation associated with the helicopter's large image surveys are consistent with and complementary to the findings of G. R. Kodikara et al. (2024), which highlighted the intensive computational demands of drone-based imaging transmission and processing in a planetary exploration context. During the simulation, the team made the decision to fly the helicopter every day, but as planning progressed, the team considered pausing flights to both assist in reducing the backlog of onboard helicopter image survey data and to wait for the rover to catch up in case the helicopter was needed to scout specific sites for the rover.

This experience suggests that the helicopter could be operated on a more strategic or "predictive" planning timeline, meaning that planning can be done in advance and does not depend as heavily on rapid science downlink assessment (L. Cheng et al. 2008; S. M. Milkovich et al. 2022). Though not as predictive as an orbiter mission, whose activities can and sometimes need to be planned months in advance, this simulation found that the helicopter could operate with a planning schedule on the order of several days to a week, which aligns generally with the cadence on which Ingenuity was operated (J. L. Anderson et al. 2023).

The mission operations team did experience some tension between the rover's demands for the helicopter's support and the helicopter's independent science objectives. The rover benefitted from keeping the helicopter relatively close (i.e., within a few hundred meters), given the helicopter's role in scouting and selecting good outcrops of high science value for the rover to study and given the potential advantage of enhanced localization offered by the helicopter's low-altitude data sets. However, the rover's near-term sol path was somewhat uncertain and more prone to being dictated by on-the-ground tactical discoveries, as evidenced by the unplanned stop at the Specialis Revelio workspace. But the helicopter's science priority during the exercise was primarily to fly over as many interesting and diverse outcrops as possible within and around the ROI. The mission team settled this tension during the simulation by choosing not to request image survey data that would enable enhanced localization for any other sites than the one the helicopter had already acquired for Godric's Hollow and doing its best to select oblique imaging sites that might be relevant for future rover planning. The team also decided to maintain its stop at Godric's Hollow in the LAP less because it was of high science priority and more because the helicopter support data existed and the time and resources that had already been invested in acquiring it. Thus, the simulation revealed that the team's selection of sites for the rover's exploration was heavily biased by the places where the helicopter had already acquired (and downlinked) data at the time operations decisions needed to be made.

5.5. Mission Simulations in the Field

Previous rover and helicopter mission analog tests have either used high-fidelity analog robotic platforms, e.g., CanMars (G. R. Osinski et al. 2019) and RAVEN (B. B. Carr et al. 2024; S. Gwizd et al. 2024; G. R. Kodikara et al. 2024), or humans in the field simulating robotic platforms (e.g., R. A. Yingst et al. 2016, 2020, 2022, R. Francis et al. 2018). An observation from the outcome of this deployment, consistent with the successful execution of the GeoHeuristic Operational Strategis (or GHOST; R. A. Yingst et al. 2016, 2020, 2022) and Rover Operations Activities for Science Team Training (or ROASTT; R. Francis et al. 2018) was that an operational field analog mission simulation can be accomplished with relatively low cost and complexity, and without the use of robotic assets, while maintaining high fidelity in operations and science decision-making. The field campaign was conducted at a site selected for its reliable, safe, and low-cost access, being reachable by ordinary road vehicles and almost completely in cellphone coverage, as well as in proximity to logistical support of a mid-sized community, only a few hours by road from the field team lead's home institution. The simplified implementation of field instruments allowed approximation of the imaging and spectrometer data from the notional Mars rover with only a few pieces of field gear, easily carried by hand and by a rented car. In particular, the decision to forego stereo imaging and communicate distances by markers in the Navcam panoramas greatly

simplified the complexity and size of the imaging systems, as well as the time and effort required for data processing and visualization. This enabled the simulation of all the rover's cameras with a single field camera and small set of lenses, which could use a lightweight tripod and manual pointing. This simple hardware made for a very portable, very reliable system which could, with sufficient operator care and expertise, produce adequately rover-like images while avoiding the time, cost, and complexity of a heavy, bulky, but more precise and repeatable custom stereo rig. Similar decisions allowed the helicopter imaging to be simulated with very simple field practices and allowed suitable spectral data to be collected with minimal complexity. This strategy of minimizing complexity while ensuring sufficient fidelity to test the questions being examined in the exercise allowed a field campaign to be conducted that was organized in a matter of weeks, with a field team deployed quickly and completing their work in only a few hours each day. This allowed responsiveness to weather and robustness to field difficulties, helping to ensure the reliable generation of decision-responsive field data, and as a result the completion of the activity.

Although this exercise demonstrated that a relatively high-fidelity, low-complexity mission simulation could be carried out without robotic facsimiles of a rover and a helicopter, the short duration of the simulation and operational constraints related to this duration limited the number of exploration scenarios, operational strategies, and sol paths that could be explored. In this simulation, the rover and helicopter were operated in the context of a single 5 sol-long mission exploration scenario using operational approaches typical of Perseverance, Curiosity, and Ingenuity, respectively, with an assumption of daily operations and payloads similar to these existing mission platforms. Furthermore, the mission operation team's decision to make use of the helicopter's enhanced localization support for the rover provided an early and impactful constraint on the helicopter's flight plans during the 5 sol simulation.

Future work could include additional simulations that explore different exploration scenarios for the rover and helicopter, including those that are lower fidelity in operational processes, timelines, and science decision-making but longer in length, do not levy specific requirements on the use of the rover's payload, do not require specific ways in which the helicopter should support rover operations, and explore various operations and nonoperations strategies for the rover and helicopter, respectively.

6. Conclusions

(1) A 5 day field and remote operations mission simulation was carried out in Rainbow Basin, California, USA to test operations strategies, science value, and challenges of a joint rover-helicopter mission architecture.
(2) Given its multi-instrument payload on the simulated mast and turret, respectively, the rover excelled at nested contextual imaging and high-resolution imaging, geochemistry, and mineralogy science observations.
(3) The helicopter excelled at the collection of vast spatial coverage of diverse terrain and geological units within a broader exploration region. Higher-resolution oblique images, rather than lower-resolution nadir-looking continuous image surveys, were the most scientifically and operationally useful data acquired by the helicopter.
(4) Given the helicopter's long flights and large-volume data products, future joint rover-helicopter missions should consider a "predictive" planning approach for helicopter operations, i.e., operating on a near-term but not daily tactical timeline. This approach would allow the mission operations team to better manage the flow of data from the mission platforms and focus tactical planning efforts on the rover.
(5) Attempts to take advantage of the helicopter's ability to aid in enhanced localization of the rover were limited by the large data volume of the image survey that needed to be downlinked, and by the mission operations team's decision to focus on a different, fortuitously encountered outcrop for detailed analysis. Enhanced localization is likely most useful in a dual-platform mission architecture if processing of the data and localization can be performed on board.
(6) The simulation showed the rover and helicopter to be complementary to each other in terms of science value, with the rover providing depth and the helicopter providing breadth to the mission's science investigation. Should such a mission architecture become possible in the future, the team should consider how best to balance the "reactive" planning needs of the rover with the more "predictive" operational cadence of the helicopter.

Acknowledgments

This study was supported by NASA PSTAR grant No. 80NSSC21K0011. Research was carried out by K.M.S., R.F., F.C., S.G., J.V., J.S., M.B., A.D., M.T., and J.O. at the Jet Propulsion Laboratory, California Institute of Technology, under a contract with the National Aeronautics and Space Administration (80NM0018D0004). C.N., J.S., R.P., and S.V. were supported by a Canadian Space Agency FAST grant (grant No. 21FAUWOB01). P.S. was supported by the Explorers Club and Fjällräven. Justin Maki assisted with parsing camera specifications and Vivian Sun assisted with spectroscopy interpretations. This manuscript was significantly improved thanks to feedback provided by two anonymous reviewers.

Appendix A
Operations Processes, Roles, and Tools

This section describes the strategic, tactical, next-day, and near-term planning processes used by the mission operations team during the mission simulation.

A.1. Operations Processes

A.1.1. Strategic Planning

The purpose of the strategic process is to develop high-level science exploration objectives, a notional traverse or flight path for the mission, and a general plan and timeline for exploration through a particular region (S. M. Milkovich et al. 2022; A. R. Vasavada 2022). This process often takes place weeks to years in advance of a mission's arrival at its exploration area and is often initiated using orbiter image data sets (S. M. Milkovich et al. 2022; V. Z. Sun et al. 2024).

The mission operations team met twice before the start of the joint rover-helicopter mission simulation to discuss the analog orbiter image data of the ROI, geologic maps

Table A1
Daily Mission Operations and Field Implementation Schedule

Team	Time[a]	Meeting
Field	8:00 a.m.–12:00 p.m.	Collection of data planned in Sol $N-1$ plan
	12:00 p.m.–2:00 p.m.	Processing and posting of decisional field data in online repository
	2:00 p.m.	Deadline for posting decisional data to online repository
Mission operations	2:00–3:00 p.m.	Optional preparation time
	3 p.m.	Start of mission operations
	3:00–3:10 p.m.	Downlink assessment of Sol $N-1$ data
	3:10–3:25 p.m.	Planning kick-off
	3:25–5:30 p.m.	Tactical (sol N) planning
	5:30–5:55 p.m.	Plan review
	5:55–6:30 p.m.	Generation of uplink products
	6:30–7:00 p.m.	Sol $N+1$ planning
	7:00–7:20 p.m.	Look Ahead Planning ($N+2$ to $N+7$)
	7:20–9:00 p.m.	Compilation of plan translation summary document, report writing, LAP refinement, margin
Field and mission operations	9:30 p.m.	Sol N plan translation tag-up between mission operations lead and field lead

Note.
[a]All times listed above are PDT.

constructed for the ROI by team members, and an initial identification and prioritization of sites of interest (Figure 2). The team first identified and discussed the geologic diversity present at the field site observed in the analog orbiter data. The team then identified sites of interest for potential rover stops and helicopter landing sites. This strategic planning discussion was used to construct a baseline Look Ahead Plan (or LAP) listing the main anticipated activities to be executed by the rover and helicopter during the 5 sol mission.

*A.1.2. Tactical (*N *Planning)*

The tactical planning process was carried out during the simulation to construct a schedule of activities for the rover and helicopter, respectively, to be carried out on Sol N (Table A1). This simulation's tactical planning process consisted of a series of meetings including "Downlink Assessment," "Planning Kick-off," "Tactical N Planning," "Plan Review," and "Generation of Uplink Products." Prior to the official start of operations, the team gathered for an optional preparation time during which the team prepared presentations and notes templates, looked briefly at any data that had been recently downlinked, and began an informal science assessment of the new data. The tactical planning process formally began with Downlink Assessment, during which the operations team reviewed which activities had been executed and completed successfully by the spacecraft during the prior day (Sol $N-1$) and verified that all expected data had been acquired and received. The team then transitioned into Planning Kick-off, during which the team discussed objectives for the N plan, key decisions for the day, and planning constraints. During the Tactical N Planning period that followed, the team reviewed new science data and discussed initial science findings from both the rover and the helicopter that might affect tactical planning and discussed a rover drive plan (including traverse path and end-of-drive position and heading) and helicopter flight plan (including flight path, landing site, and mid-flight imaging locations). The team also selected science activities from a predetermined list of approved activities (Tables A2 and A3) and selected specific targets for those activities. The team typically constructed the rover plan first, since it was more complex and required more team discussion. A short Plan Review meeting followed Tactical N Planning, during which the plans for both the rover and helicopter were reviewed activity by activity and checked to ensure that both plans fit within the stated resource allocations for duration, data volume, and energy. The team also reviewed the data downlink prioritization plan and verified which data products were expected in time for the next day's planning. Tactical planning concluded with a final poll of all roles for concurrence and was followed by a short work period, "Generation of uplink products," during which team members prepared image annotations of the rover traverse and science targets, as well as helicopter flight paths, imaging locations, and landing sites to be passed to the field team (Table A1).

Staggered scheduling of the science operations and field activities allowed a daily cadence in which the mission operations team would prepare a plan and "uplink" the requested set of rover and helicopter activities to the field team. The field team would then collect observations during local daylight at the field site, process them as necessary, and send them as a "downlink" package in a network filesharing system in time for the next mission operations planning session.

For the rover, the mission operations team built daily activity plans beginning with one of four prebuilt plan templates: (1) a maximum drive plan consisting of the longest drive that resources or simulation constraints allowed with minimum post-drive engineering and science workspace imaging to enable the next sols planning; (2) a remote-sensing plus drive plan consisting of several LIBS/VISIR/RMI and Mastcam mosaic placeholders, followed by a drive and post-drive engineering and science imaging; (3) a proximity science plan consisting of Raman and XRF spectroscopy, Turretcam imaging, and placeholder LIBS/VISIR/RMI and Mastcam observations; and (4) an abrasion plan including an abrasion plus Turretcam imaging and placeholder LIBS/VISIR/RMI and Mastcam observations. The use of these templates was not intended to constrain the science activity choices of the mission operations team, but rather to serve as a starting point

Table A2
Rover Science and Engineering Activities and Resources

Type	Activity	Duration (minutes)	Data Volume (Mbits)	Energy (Wh)	Notes
Science	LIBS 3 points	7	48	6	…
	LIBS 5 points	12	80	10	…
	LIBS 10 points	20	160	20	…
	VISIR 3 points	7	48	6	…
	VISIR 5 points	12	80	10	…
	VISIR 10 points	20	160	20	…
	RMI Image	1	16	2	…
	AEGIS Analysis	5	8	2	…
	Navcam Panorama	25	160	25	…
	Mastcam Workspace PDI	8	216	14	…
	Mastcam Clast Survey	3	48	4	…
	Mastcam - Z30	3	36	4	One frame
	Mastcam - Z100	3	36	4	One frame
	XRF Daytime Short 15 minutes	45	2.4	7	…
	XRF Daytime Medium 90 minutes	90	4	14	…
	XRF Overnight 12 hr	60	8	100	…
	Raman Short	45	9.6	25	…
	Raman Long	90	16	40	…
	Turretcam Single Image	4	48	4	…
	Turretcam Suite (25, 5, 2 cm standoffs)	8	144	8	…
	Turretcam Mosaic	10	192	10	4 × 15 cm standoff
Engineering	Rover Traverse Autonav Drive	55	16	40	10 m drive
	Rover Traverse Directed Drive	35	8	40	10 m drive
	LIBS/VISIR/RMI Power ON	10	0.72	4	…
	LIBS/VISIR/RMI Power OFF	4	0.08	1	…
	Arm - Unstow	20	4	45	…
	Arm - Stow	20	4	45	…
	Arm - Move	10	4	30	…
	Arm - Place on target	10	4	20	…
	Arm - Instrument Swap	10	1.6	15	…
	Abrasion/Dust Removal Tool	90	4	100	…

Table A3
Helicopter Science and Engineering Activities and Resources

Type	Activity	Duration (minutes)	Data Volume (Mbit)	Energy (Wh)	Notes
Science	Low-altitude survey	0.83	1200	4.86	50 m flight
	High-altitude survey	0.42	150	2.78	50 m flight
	Oblique camera image	0.5	48	4	…
	Landed nadir camera image	0.5	48	4	…
	Landed VISIR	4	64	10	…
Engineering	Heli start-up	0.5	1.2	8	…
	Heli ascent	0.25	40	0.49	5 m ascended
	Heli descent	0.25	40	0.49	5 m descended
	Rapid traverse (no imaging)	0.42	40	2.1	50 m flight
	Heli shutdown	0.5	1.2	4	…

to make plan construction easier for the Science Planner. These templates could be fully modified to add or remove activities (Table A2), specify the length of a drive, set the number of frames in a mosaic, or the length of a proximity instrument scan (e.g., long or short). Proximity science could be added before the drive in the drive plan templates, pending resource availability. To increase the fidelity of the simulation's resource modeling, the duration, data volume, and energy of engineering activities such as "LIBS/VISIR/RMI Power ON" and "LIBS/VISIR/RMI Power OFF," as well as rover arm stow, unstow, placement, moves, and instrument swap activities were accounted for in the plan (Table A1).

For the helicopter, the mission operations team approached daily activity planning in a similar way as for the rover but using a single plan template. A typical helicopter plan included resource accounting for engineering activities such as helicopter start-up at the beginning of each plan, ascents and descents, and shutdown at the end of each plan (Table A2 and C2).

Between the start-up and shutdown activities, the mission operations team had the flexibility to determine the path of the flight, including options for a low-altitude survey, high-altitude survey, or a rapid traverse with no imaging (Table A3). Optional activities included low-altitude oblique imaging or landed single-point VISIR and imaging observations book-kept at the conclusion of the flight plan (Table A3).

A.1.3. Next Day (N + 1) and Near-term (N + 2 to N + 7) Planning

Following the conclusion of the tactical planning process, the team met to discuss the $N + 1$ plan, including science objectives of the plan at a high level, selection of a sol template, and population of the plan with any known science activities, parameters or targets, if known in advance. The team also worked on preliminary sketches of a drive path for the rover and a flight path for the helicopter so that resources could be reviewed. $N + 1$ planning was carried out with the expectation that the plan would be significantly refined the following day in response to the most recent downlinked decisional data.

Once an $N + 1$ plan had been constructed, the team participated in an LAP meeting during which a spreadsheet containing an overview of the Sol $N + 2$ to $N + 7$ plans was book-kept (e.g., Table 2). The team reviewed the next 5 sols of activities at a high level, discussing which sites of interest the rover or helicopter would likely explore next and which main activities would likely populate the plan.

A.2. Operations Roles

The mission operations team consisted of six roles staffed daily throughout the duration of the mission simulation: Science Lead, Science Planner, Target and Mobility Specialist, Helicopter Representative, Documentarian, and multiple Support Scientists. Members of the mission operations team rotated through these roles over the course of the 5 day simulation, with team members typically filling a certain role for 2–3 consecutive days before transitioning to a different role.

The Science Lead's responsibilities included leading the mission operations team to consensus decisions regarding rover and helicopter activity and target selection, and ensuring that the operations team followed the meeting timeline and agendas during planning. The Science Planner was responsible for displaying and editing the N, $N + 1$, and Look Ahead activity plans for the rover and helicopter during daily planning. They were also responsible for verifying that each plan satisfied known data volume, plan duration, and energy constraints. The Science Planner tracked the downlink status of acquired science data and prepared a downlink plan for the upcoming sol or sols. The Target and Mobility Specialist was responsible for sketching out a daily drive path for the rover that met safety and hazards constraints, particularly related to slope and obstacles visible in helicopter or analog orbiter image data. They were responsible for annotating a drive path that included the start and end positions and headings of the planned drive as well as the location of mid-drive observation stops. The Targeting and Mobility Specialist was also responsible for annotating the rover's Navcam images to show the location and extent of requested rover observations, including specific target locations and approximate image and mosaic footprints. The Targeting and Mobility specialist also participated in science discussions related to target selection and end-of-drive positioning.

The Helicopter Representative was responsible for planning a daily flight path for the helicopter that met constraints for safe landing, including a proposal for oblique imaging locations and image survey mode. The Helicopter Representative was also responsible for proposing and prioritizing helicopter data from previous flights for downlink during the planning sol. The Helicopter Representative worked largely independently to come up with a proposal for the helicopter's daily activities that was then presented to the full mission operations group for discussion and refinement.

The Documentarian was responsible for keeping a daily written record of the planning process including a description and justification of major activity planning or targeting decisions. This role also functioned as a general science team member contributing to discussions of recent data and proposing science observations and targets. The Support Scientist role participated in all tactical, $N + 1$, and LAP discussions, reviewed the most recent downlinked data, prepared a short summary presentation of science results from the previous sol or newly downlinked data, and proposed targets and observations for the tactical, $N + 1$, and LAP plans.

A.3. Operations Tools

Daily tactical N, $N + 1$, and LAP plans for the rover and helicopter were constructed in spreadsheet templates, while planning kick-off and data analysis slide presentations were constructed and updated daily. These spreadsheets and slide presentations, along with mission data and Documentarian notes, were all stored within the team network filesharing system.

The analog orbiter raster data sets used by the team during strategic planning were converted into Tile Map Service tiles and imported into a Multi-Mission Geographic Information System (MMGIS; F. J. Calef et al. 2023). This tool was built for the NASA Advanced Multi-Mission Operations System, which support missions with operational tools (F. J. Calef et al. 2023). This software is free and open source, available in a public code repository (F. J. Calef et al. 2024) and utilized on several planetary and Earth science missions. In addition to its use during strategic planning for geologic analysis of the field site and initial mission planning, the team's MMGIS application was also used daily during the mission simulation to map the planned rover traverse and helicopter flight paths and view helicopter image data once downlinked. Once planning was complete, maps of the planned rover traverse, helicopter flight, and points of interest were captured from the application and transmitted to the field team.

Appendix B
2018 Rainbow Basin UAS Campaign

Figure B1 shows the flight plain, orthomosaic, and data products derived from the 2018 UAS imaging campaign in Rainbow Basin. This data set was the source data for the simulated orbiter HiRISE images and the helicopter high-altitude and low-altitude images used in the joint helicopter-rover mission simulation.

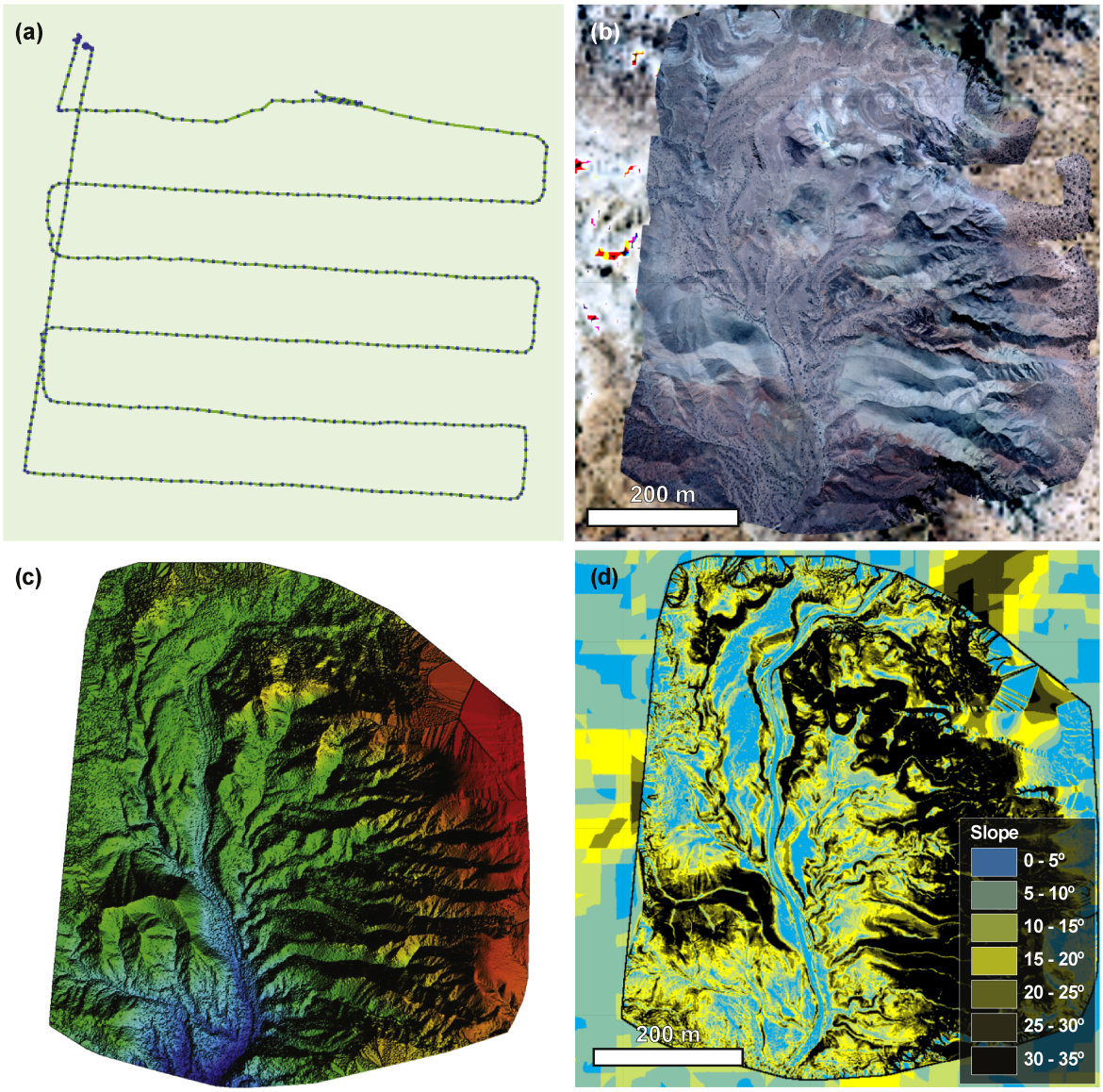

Figure B1. 2018 Rainbow Basin UAS image acquisition and derived data products for the ROI. (a) Image locations collected from the UAS in flight at Rainbow Basin. (b) Analog HiRISE orthomosaic of the Rainbow Basin field site. (c) DEM of the processed UAS images. (d) 1 m slope map derived from the UAS DEM.

Appendix C
Detailed Mission Narrative

Table C1 contains a list of all rover activities planned during the mission simulation, along with duration, data volume, energy, and planning details associated with each activity. Table C2 contains a list of all helicopter activities planned during the mission simulation, along with duration, data volume, energy, elevation, and flight distance.

Table C1
All Rover Activities by Sol

Sol	Type	Description	Duration (minutes)	Data Volume (Mbit)	Energy (Wh)	Frames	Drive Distance (m)
100	LIBS 5 points	AEGIS target	…	…	…	…	…
100	VISIR 5 points	AEGIS target	…	…	…	…	…
100	RMI Image	AEGIS target	…	…	…	…	…
100	Navcam Panorama	Navcam 360 PDI Pano	…	…	…	…	…
100	MastCam Mosaic - Workspace PDI	N/A	…	…	…	…	…
101	LIBS/VISIR/RMI Power ON	N/A	10	0.72	4	…	…
101	RMI Image	RMI 4 × 1 of red-toned bedrock wall Durmstrang	1	16	2	…	…
101	RMI Image	RMI 4 × 1 of red-toned bedrock wall Durmstrang	1	16	2	…	…
101	RMI Image	RMI 4 × 1 of red-toned bedrock wall Durmstrang	1	16	2	…	…
101	RMI Image	RMI 4 × 1 of red-toned bedrock wall Durmstrang	1	16	2	…	…
101	VISIR 5 points	Mudcracks at Hippogriff traget	12	80	10	…	…
101	RMI Image	Hippogriff target	1	16	2	…	…
101	LIBS/VISIR/RMI Power OFF	N/A	4	0.08	1	…	…
101	Mastcam Mosaic - Z30	ZCAM doc of Hippogriff mudcrack target	3	36	4	1	…
101	Mastcam Mosaic - Z100	ZCAM 2 × 1 of boulder-bearing target Ironbelly	4	72	6	2	…
101	Rover Traverse - Autonav Drive	79 m drive to Spinner's End	296.5	126.4	316	…	79
101	Navcam Panorama	NCAM PDI Pano AZ 230–60	25	160	25	…	…
102	LIBS/VISIR/RMI Power ON	N/A	10	0.72	4	…	…
102	RMI Image	5 × 1 RMI mosaic on red layered target Alohomora	1	16	2	…	…
102	RMI Image	5 × 1 RMI mosaic on red layered target Alohomora	1	16	2	…	…
102	RMI Image	5 × 1 RMI mosaic on red layered target Alohomora	1	16	2	…	…
102	RMI Image	5 × 1 RMI mosaic on red layered target Alohomora	1	16	2	…	…
102	RMI Image	5 × 1 RMI mosaic on red layered target Alohomora	1	16	2	…	…
102	VISIR 5 points	Lumos white patch at Grimmauld Place	12	80	10	…	…
102	RMI Image	5 × 1 RMI mosaic of Lumos	1	16	2	…	…
102	RMI Image	5 × 1 RMI mosaic of Lumos	1	16	2	…	…
102	RMI Image	5 × 1 RMI mosaic of Lumos	1	16	2	…	…
102	RMI Image	5 × 1 RMI mosaic of Lumos	1	16	2	…	…
102	RMI Image	5 × 1 RMI mosaic of Lumos	1	16	2	…	…
102	LIBS/VISIR/RMI Power OFF	N/A	4	0.08	1	…	…
102	Rover traverse - Autonav drive	60 m drive to Grimmauld Place with mid-drive imaging after 26.5 m of driving	230	96	240	…	60
102	Mastcam Mosaic - Z30	6 × 1 mid-drive mosaic of young fluvial deposits at target Invisibility_Cloak	8	216	14	…	6
102	Navcam Panorama	Navcam 360 PDI Pano	25	160	25	…	…
102	LIBS/VISIR/RMI Power ON	N/A	10	0.72	4	…	…
102	AEGIS Analysis	White unit exposed at Grimmauld Place	5	8	2	…	…
102	LIBS 5 points	AEGIS target	12	80	10	…	…
102	VISIR 5 points	AEGIS target	12	80	10	…	…
102	RMI Image	AEGIS target	1	16	2	…	…
102	LIBS/VISIR/RMI Power OFF	N/A	4	0.08	1	…	…
102	Mastcam Mosaic - Z100	1 × 1 of AEGIS target	3	36	4	…	1
102	Mastcam Mosaic - Z100	6 × 2 untargeted mosaic of the base of Grimmauld Place slope	14	432	26	…	12
103	Arm - Unstow	N/A	20	4	45	…	…
103	Arm - Place on target	N/A	10	4	20	…	…
103	Turretcam Standard Suite (25, 5, 2 cm standoff)	Representative bedrock target Fizzing_Whizbees	8	144	8	…	…
103	Arm - Instrument Swap	N/A	10	1.6	15	…	…
103	PIXL - Daytime Short 45 min	Representative bedrock target Fizzing_Whizbees	45	2.4	7	…	…
103	Arm - Place on Target	N/A	10	4	20	…	…
103		Light-toned nodule target Twilfitt_and_Tattings	8	144	8	…	…

Table C1
(Continued)

Sol	Type	Description	Duration (minutes)	Data Volume (Mbit)	Energy (Wh)	Frames	Drive Distance (m)
	Turretcam Standard Suite (25, 5, 2 cm standoff)						
103	Arm - Instrument Swap	N/A	10	1.6	15	…	…
103	PIXL - Daytime Short 45 min	Light-toned nodule target Twilfitt_and_Tattings	45	2.4	7	…	…
103	Arm - Stow	N/A	20	4	45	…	…
103	LIBS/VISIR/RMI Power ON	N/A	10	0.72	4	…	…
103	LIBS 5 points	Brown nodule target Bludger	12	80	10	…	…
103	VISIR 5 points	Brown nodule target Bludger	12	80	10	…	…
103	RMI Image	Brown nodule target Bludger	1	16	2	…	…
103	LIBS 5 points	Green bedrock target Venemous_Tentacula	12	80	10	…	…
103	VISIR 5 points	Green bedrock target Venemous_Tentacula	12	80	10	…	…
103	RMI Image	Green bedrock target Venemous_Tentacula	1	16	2	…	…
103	LIBS/VISIR/RMI Power OFF	N/A	4	0.08	1	…	…
103	Mastcam Mosaic - Z100	3 × 3 mosaic of outcrop Specialis_Revelio, including LIBS/VISIR/RMI targets Bludger and Venemous_Tentacula	11	324	20	9	…
103	Rover Traverse - Directed Drive	N/A	15	1.6	8	…	2
103	Navcam Panorama	Navcam 360 PDI Pano	25	160	25	…	…
103	MastCam Mosaic - Workspace PDI	N/A	8	216	14	…	…
103	LIBS/VISIR/RMI Power ON	N/A	10	0.72	4	…	…
103	AEGIS Analysis	AEGIS of rock target	5	8	2	…	…
103	LIBS 5 points	N/A	12	80	10	…	…
103	VISIR 5 points	N/A	12	80	10	…	…
103	RMI Image	N/A	1	16	2	…	…
103	LIBS/VISIR/RIM Power OFF	N/A	4	0.08	1	…	…
103	MastCam Mosaic - Z100	AEGIS doc image	3	36	4	1	…
104	Arm - Unstow	N/A	20	4	45	…	…
104	Arm - Place on Target	Target Bludger	10	4	20	…	…
104	Rock Abrasion/DRT	Target Bludger	90	4	35	…	…
104	Arm - Instrument Swap	N/A	10	1.6	15	…	…
104	Turretcam Standard Suite (25, 5, 2 cm standoff)	Target Bludger	8	144	8	…	…
104	Arm - Instrument Swap	N/A	10	1.6	15	…	…
104	PIXL - Daytime Short 45 min	Target Bludger	45	2.4	7	…	…
104	Arm - Instrument Swap	N/A	10	1.6	15	…	…
104	Prox Raman - Short	Target Bludger	45	9.6	25	…	…
104	Arm - Place on Target	Target Fizzing_Whizbees	10	4	20	…	…
104	Prox Raman - Short	Target Fizzing_Whizbees	45	9.6	25	…	…
104	Arm - Stow	N/A	20	4	45	…	…
104	MastCam Mosaic - Z100	4 × 2 diagonal mosaic of the lower Specialis_Revelio workspace	10	288	18	8	…
104	LIBS/VISIR/RMI Power ON	N/A	10	0.72	4	…	…
104	LIBS 5 points	Diagonal raster on target Beauxbatons	12	80	10	…	…
104	RMI Image	Target Beauxbatons	1	16	2	…	…
104	LIBS/VISIR/RMI Power OFF	N/A	4	0.08	1	…	…
105	Mastcam Mosaic - Z100	Documentation of LIBS target Beauxbatons	3	36	4	1	…
105	Rover Traverse - Autonav drive	83 m precision drive to Godric's Hollow; mid-drive imaging after 73 m	310.5	132.8	332	…	83
105	Mastcam Mosaic - Z30	10 m before EOD; Z30 3 × 2 mosaic of Godric's Hollow approaching Bloody Baron	8	216	14	6	…
105	Navcam Panorama	270 NCAM PDI Pano (Rover Az Clockwise 180–90)	18.75	120	18.75	…	…

Table C2
All Helicopter Activities by Sol

Sol	Type	Description	Duration (minutes)	Data Volume (Mbit)	Energy (Wh)	Elevation (m)	Flight Distance (m)
101	Heli start-up	N/A	0.5	1.2	8.0	…	…
101	Heli ascent	N/A	1.0	160	1.9	20	…
101	Heli survey traverse high altitude	High-altitude survey traverse of Spinner's End and Grimmauld Place	2.0	726	13.4	…	242
101	Heli descent	N/A	0.5	80	1.0	−10	…
101	Heli survey traverse low altitude	Low-altitude survey traverse of Godric's Hollow 1/2	0.5	744	3.0	…	31
101	Heli descent	N/A	0.4	56	0.7	−7	…
101	Oblique camera image	Image of Godric's Hollow abrasion site from 3 m altitude - southeast (163° CW)	0.5	48	4.0	…	…
101	Oblique camera image	Image of Godric's Hollow from 3 m altitude - northeast (39° CW)	0.5	48	4.0	…	…
101	Heli ascent	Ascend back to 10 m	0.4	56	0.7	7	…
101	Heli survey traverse low altitude	Low-altitude survey traverse of Godric's Hollow 2/2	0.2	312	1.3	…	13
101	Heli descent	Descent 7 m	0.4	56	0.7	−7	…
101	Oblique camera image	Image of Flutterby_Bush: Godric's Hollow landing site to the north	0.5	48	4.0	…	…
101	Heli descent	N/A	0.2	24	0.3	−3	…
101	VISIR measurement	VISIR measurement of Flutterby_Bush (at Godric's Hollow landing site)	4.0	64	10.0	…	…
101	Nadir camera image	Nadir image of VISIR target Flutterby_Bush (at Godric's Hollow landing site)	0.5	48	4.0	…	…
102	Heli start-up	N/A	0.5	1.2	8.0	…	…
102	Heli ascent	N/A	0.2	24	0.3	3	…
102	Oblique camera image	Oblique camera image of the Godric's Hollow region to the northeast	0.5	48	4.0	…	…
102	Heli ascent	N/A	0.9	136	1.7	17	
102	Heli survey traverse high altitude	High-altitude survey traverse of Knockturn Alley, Forbidden Forest	2.5	900	16.7	…	300
102	Heli descent	N/A	0.9	136	1.7	−17	…
102	Oblique camera image	Oblique camera image of the Cleansweep landing site to the south	0.5	48	4.0	…	…
102	Heli descent	N/A	0.2	24	0.3	−3	…
102	VISIR measurement	VISIR of heli Sol 102 landing site: Cleansweep	4.0	64	10.0	…	…
102	Nadir camera image	Doc image of heli Sol 102 landing site: Cleansweep	0.5	48	4.0	…	…
102	Heli shutdown	N/A	0.5	1.2	4.0	…	…
103	Heli start-up	N/A	0.5	1.2	8.0	…	…
103	Heli ascent	N/A	0.5	80	1.0	10	…
103	Heli survey traverse low altitude	Low-altitude survey of Godric's Hollow/Hogsmeade (1/2)	1.2	1776	7.2	…	74
103	Heli descent	N/A	0.4	56	0.7	−7	…
103	Oblique camera image	Image looking southeast Godric's Hollow	0.5	48	4.0	…	…
103	Heli ascent	N/A	0.4	56	0.7	7	…
103	Heli survey traverse low altitude	Low-altitude survey of Godric's Hollow/Hogsmeade (2/2)	0.9	1296	5.3	…	54
103	Heli descent	N/A	0.4	56	0.7	−7	…
103	Oblique camera image	Image looking north-northwest at Hogsmeade	0.5	48	4.0	…	…
103	Heli ascent	N/A	0.9	136	1.7	17	…
103	Heli survey traverse high altitude	High-altitude survey of Hogsmeade/The Burrow	1.4	504	9.3	…	168
103	Heli descent	N/A	0.9	136	1.7	−17	…
103	Oblique camera image	Oblique camera image looking west at The Burrow landing site Chizpurfle	0.5	48	4.0	…	…
103	Oblique camera image	Oblique camera image looking north at The Burrow landing site Chizpurfle	0.5	48	4.0	…	…
103	Oblique camera image	Oblique camera image looking east at The Burrow landing site Chizpurfle	0.5	48	4.0	…	…
103	Heli descent	N/A	0.2	24	0.3	−3	…
103	VISIR measurement	VISIR measurement at The Burrow landing site Chizpurfle	4.0	64	10.0	…	…

Table C2
(Continued)

Sol	Type	Description	Duration (minutes)	Data Volume (Mbit)	Energy (Wh)	Elevation (m)	Flight Distance (m)
103	Nadir camera image	Nadir camera image at The Burrow landing site Chizpurfle	0.5	48	4.0	…	…
103	Heli shutdown	N/A	0.5	1.2	4.0	…	…
104	Heli start-up	N/A	0.5	1.2	8.0	…	…
104	Heli ascent	N/A	0.5	80	1.0	10	…
104	Heli survey traverse low altitude	Low-altitude survey traverse of the Burrow	2.5	3528	14.3	…	147
104	Heli descent	N/A	0.4	56	0.7	−7	…
104	Oblique camera image	Oblique image looking west at landing site	0.5	48	4.0	…	…
104	Heli descent	Landing site at Charing Cross Road at Bubotuber	0.2	24	0.3	−3	…
104	Nadir camera image	Nadir image of landing site Bubotuber	0.5	48	4.0	…	…
104	Heli Shutdown	N/A	0.5	1.2	4.0	…	…
105	Heli Startup	N/A	0.5	1.2	8.0	…	…
105	Heli ascent	N/A	0.5	80	1.0	10	…
105	Heli survey traverse low altitude	Low-altitude survey of Azkaban	1.3	1824	7.4	…	76
105	Heli descent	N/A	0.4	56	0.7	−7	…
105	Oblique camera image	Oblique looking northwest (Az 315) to Owlery	0.5	48	4.0	…	…
105	Heli ascent	N/A	0.4	56	0.7	7	…
105	Heli survey traverse low altitude	Low-altitude survey along Azkaban	2.1	3000	12.2	…	125
105	Heli descent	N/A	0.4	56	0.7	−7	…
105	Oblique camera image	Oblique looking northwest (Az 265) to Azkaban	0.5	48	4.0	…	…
105	Heli ascent	N/A	0.4	56	0.7	7	…
105	Heli survey traverse low altitude	Flying back to Bubotuber	1.6	2304	9.3	…	96
105	Heli descent	N/A	0.5	80	1.0	−10	…
105	Heli shutdown	N/A	0.5	1.2	4.0	…	…

C.1. Sol 101

The mission simulation officially began on Sol 101, following a ∼100 sol commissioning phase in which it was assumed that the rover's payload had been tested, and that the helicopter had performed a series of local test flights. The team began the exercise with Sol 100 rover data in hand, including a Navcam mosaic (Figure 4(a)), a Mastcam clast survey, and LIBS, VISIR, and RMI from an AEGIS target. The team planned a 79 m drive for the rover to the north through Diagon Alley toward Spinners End (Figure 3(a)). This location was selected as the end-of-drive target to enable near- to midfield remote sensing on the reddish bedrock of the Spinners End slope. A pre-drive remote-sensing block included VISIR, RMI, and Mastcam on mudcracks (target "Hippogriff") in the workspace (Figure 4(b)), a Mastcam mosaic of boulder-bearing fluvial deposits in the midfield, and a long-distance RMI mosaic targeting capping bedrock to the southeast of the rover (Figure 4(g)).

The helicopter plan for Sol 101 included a ∼285 m-long high-altitude survey flight over Spinners End and Grimmauld Place, then heading toward Godric's Hollow (Figure 3(b)). Thirty meters from the anticipated rover proximity science location at Godric's Hollow, the helicopter was directed to descend for the requisite low-altitude survey that would enable the rover's enhanced localization during its future approach to the site (Figure 3(b)). Near the conclusion of the flight, the helicopter acquired two oblique images, one to the north and one to the south, to image two candidate abrasion locations (Figure 3(b)). The helicopter then landed at a site called Flutterby Bush. The helicopter acquired another oblique image during its descent and a VISIR and nadir image upon landing (Table C2).

The rover's remote-sensing observations and the helicopter's imaging survey flights were data intensive, so only the following data products could be included in the Sol 102 decisional downlink (Table A1): 180° of the post-drive Navcam to enable the next sol's rover drive, 15 m of the low-altitude helicopter survey approach to Godric's Hollow, and the two oblique helicopter images of the candidate proximity science sites. The low-altitude survey data were prioritized to enable the rover's future approach to the abrasion site, and the oblique images were selected to enable team discussion of the preferred abrasion site.

C.2. Sol 102

The Sol 101 drive ended with the rover very near the transition between the reddish rocks of Spinners End and the white slope of Grimmauld Place (Figure 3(a)). This enabled pre-drive remote sensing including a VISIR observation and RMI mosaic on the target Lumos, a midfield observation of a light-toned patch on the lower slopes of Grimmauld Place (Figure 4(f)), and an RMI mosaic on the bedrock layers exposed in the upper slope of Spinners End. This was followed by a 60 m drive continuing north toward the base of

Grimmauld Place (Figure 3(a)). Post-drive observations included a Navcam workspace mosaic, Grimmauld Place Mastcam imaging, and an autonomously targeted AEGIS bedrock target at the base of Grimmauld Place.

Having acquired the low-altitude survey of the approach to Godric's Hollow in the previous sol's plan, the helicopter was free to explore further afield to the east and north of the exploration area. The Sol 102 plan for the helicopter included a departure from Flutterby Bush, with an oblique image acquired during the initial ascent. The helicopter then flew to the southeast through Knockturn Alley, then flew north-northwest to the boundary of a gray and white layered sequence at Forbidden Forest (Figure 3(b)). Finally, the helicopter headed northwest to its landing site at Cleansweep, a site with apparently massive greenish-gray bedrock (Figure 3(b)). An oblique image was planned during the descent to Cleansweep, and VISIR and a nadir image were acquired after landing.

The only data downlinked in the decisional pass during this sol were the rover's Sol 102 post-drive Navcam mosaic to enable drive planning for the next day and the remaining 15 m of the Sol 101 low-altitude helicopter survey to cover the approach to the rover's future proximity science target at Godric's Hollow (Table 3).

C.3. Sol 103

Sol 103 brought a surprising tactical plan change for the rover. Originally, the team had anticipated using the Sol 103 rover plan for very minimal pre-drive remote sensing followed by a long drive to the Godric's Hollow proximity science site, enabled by the low-altitude helicopter survey. However, the layered, fine-grained outcrop that the rover found itself in front of at the start of Sol 103 planning, named Specialis Revelio, was deemed scientifically important enough that the team decided to remain at this site (Figure 5). The team planned proximity science (XRF and Turretcam on two targets, layered green bedrock at Fizzing Whizbees and light-toned bedrock at Twilfitt and Tattings; Figure 5). The team then planned LIBS, VISIR, and RMI on a green layered target, Venomous Tentacula, and Bludger, a freshly broken nodule (Figure 5(b)). Pre-drive science was followed by a 2 m bump to center the Bludger nodule in the workspace to prepare for abrasion and proximity science on Sol 104 since Bludger, which the team speculated could be a carbonate or silica nodule of astrobiological significance, was unreachable by the arm from the rover's Sol 103 position.

The Sol 103 helicopter plan was unaffected by the surprise outcrop encountered by the rover, and the helicopter continued its exploration with a ∼294 m-long flight through unexplored terrains to the north (Figure 3(b)). From the Cleansweep landing site, the helicopter then flew a low-altitude survey to the southwest and acquired an oblique image over the northern side of Godric's Hollow, where analog orbiter image data showed layered bedrock and complex structural relationships. The helicopter then continued its flight at high altitude toward a site called Hogsmeade where white and tan bedrock was exposed (Figures 3 and 4(b)). Following an oblique image at Hogsmeade, the helicopter continued northwest toward a landing site at Chizpurfle, in an area named The Burrow and characterized by low rolling hills exposing layered gray, white, and red bedrock (Figures 3 and 4(b)). Three oblique images looking west, north, and east were acquired during the descent to Chizpurfle.

The team used its daily decisional downlink budget to return rover observations from the Specialis Revelio workspace to enable follow-up activities the next day. No helicopter data were downlinked (Table A1).

C.4. Sol 104

The rover remained at the Specialis Revelio workspace on Sol 104 for further remote sensing and proximity science. The rover acquired proximity science data on the nodule target Bludger (Turretcam, XRF, Raman) and the Fizzing Whizbees bedrock target (Raman; Figure 5(c)). The team also planned LIBS, RMI, and Mastcam on reddish layers at the target Beauxbatons and a Mastcam mosaic to aid in building the stratigraphic context for the Specialis Revelio workspace.

The helicopter's Sol 104 plan included a ∼147 m flight to the west, taking off from the Chizpurfle landing site and landing at Bubotuber, a location that would enable future exploration in the northwest quadrant of the ROI (Figure 3(b)). The team favored a low-altitude survey over the layered deposits, ending the flight with the acquisition of an oblique image just prior to landing. The team planned for a landing image but declined a landed VISIR observation since the orbiter image data showed the area to be unconsolidated alluvium and a large backlog of helicopter data remained on board. The Sol 104 decisional downlink included almost all the rover data (except the Beauxbaton RMI mosaic) and no helicopter image data (Table A1).

C.5. Sol 105

Following two sols spent at Specialis Revelio, the rover resumed its traverse toward Godric's Hollow and the Bloody Baron proximity science workspace as originally planned (Table 2). Since the low-altitude survey covering the last 30 m approach to Bloody Baron was downlinked several sols prior, the team planned an ∼83 m precision drive to the proximity science workspace, avoiding the need for a bump sol (Figure 3(a)). Given the length of the drive, pre-drive remote sensing was limited. Before reaching Godric's Hollow, the team planned a mid-drive imaging stop to acquire Mastcam context of the proximity science location. Resources allowed only a limited partial Navcam post-drive mosaic.

The helicopter plan consisted of an ∼297 m circular survey flight at low altitude taking off from and returning to the Bubotuber site (Figure 3(b)). This loop was intended to give the team a better understanding of the sedimentary sequence at Azkaban in hopes of correlating stratigraphy across Diagon Alley. Returning to the Bubotuber landing site also allowed first characterization of Azkaban while leaving open the possibility of returning to the Chamber of Secrets or Forbidden Forest regions in subsequent flights. During its flight, the helicopter made an oblique imaging stop ∼76 m into the flight toward the southwest at a site called Owlery (Figure 3(b)). After flying 125 m to the north, the helicopter descended again for another oblique imaging stop at the base of layered outcrops exposed at Azkaban. The helicopter then flew the remaining 96 m back toward Bubotuber (Figure 3(b)). No VISIR or landed images were acquired since the helicopter had already been to this site.

The helicopter's oblique images were prioritized for the Sol 105 decisional downlink, including the Sol 101 image of Flutterby Bush, the Sol 103 image of Chizpurfle, and the Sol

105 oblique images of Owlery and layers at Azkaban. The team also downlinked the Sol 105 rover image data (Table A1).

C.6. Sol 106–110 Look Ahead Plan

On Sol 105, the last day of the mission simulation, the team carried out a typical LAP meeting to sketch out a plan for Sols 106–110 (Table 2). Having just arrived at the Bloody Baron workspace following the Sol 105 precision drive, the team anticipated spending Sol 106 executing an abrasion followed by proximity science and remote sensing. The team planned for the rover to depart Bloody Baron on Sol 107, driving toward Hogsmeade (Figure 3(a)). Since the low-altitude image survey covering the approach to Hogsmeade had not yet been downlinked as of the LAP meeting on Sol 105, the team assumed a bump would be needed on Sol 108 to position the rover at a proximity science workspace at Hogsmeade. However, the team could decide to downlink this image survey on Sol 106 to enable this future precision drive and eliminate the need for a bump sol. On Sol 109 the team planned an abrasion, proximity science, and remote sensing at Hogsmeade, followed by a drive toward The Burrow on Sol 110.

On Sol 106, the team would fly the helicopter along the edge of The Burrow, acquiring oblique images of potential outcrops accessible to the rover. On Sols 107 and 108, the helicopter would fly into The Burrow, acquiring image surveys, oblique images, and landing observations at a minimum of two sites within this region. On Sol 109, the helicopter would head northwest into Azkaban performing an image survey, oblique imaging, and landed science here. Sol 110 would see the helicopter embark on a flight toward a new, yet-to-be determined ROI.

Appendix D
Science Data Downlink Schedule

Table D1 provides the data downlink schedule and status of all rover and helicopter activities acquired during the mission simulation.

Table D1
Science Data Downlink Schedule

Planning Sol	Vehicle	Instrument	Activity/Target	Data Volume (kB)	Decisional Downlink on Sol Acquired	Sol Downlinked					End-of-exercise Downlink Pass	Remaining Onboard Indefinitely
						101	102	103	104	105		
101	Rover	Mastcam	Hippogriff M-30	36	No	…	Complete	…	…	…	…	…
		Mastcam	Ironbelly M-100	72	No	…	…	…	…	…	Complete	…
		RMI	Hippogriff	16	No	…	Complete	…	…	…	…	…
		RMI	Durmstrang	64	No	…	…	…	…	…	Complete	…
		VISIR	Hippogriff	80	No	…	Complete	…	…	…	…	…
		Navcam	PDI 360 pano	160	Partial	180°	…	…	…	…	180°	…
	Heli	Survey inflight imager	High altitude (242 m)	726	No	…	…	…	…	…	60 m	182 m
		Survey inflight imager	Low altitude (44 m)	1056	Partial	15 m	16 m	…	…	…	…	13 m
		Oblique image	Viewpoint 1	48	Yes	Complete	…	…	…	…	…	…
		Oblique image	Viewpoint 2	48	Yes	Complete	…	…	…	…	…	…
		Oblique image	Landing site (Flutterby Bush); north direction	48	No	…	…	…	…	Complete	…	…
		VISIR	Landing site (Flutterby Bush)	64	No	…	…	…	…	…	Complete	…
		Landed image	Landing site (Flutterby Bush)	48	No	…	…	…	…	…	Complete	…
102	Rover	RMI	Alohomora	80	No	…	…	…	…	…	Complete	…
		RMI	Lumos	80	No	…	…	…	…	…	Complete	…
		VISIR	Lumos	80	No	…	…	…	…	…	Complete	…
		Navcam	PDI 360 pano	160	Yes	…	Complete	…	…	…	…	…
		Mastcam	Mid-drive Z30 6 × 1 Invisibility Cloak cliff	216	No	…	…	…	…	…	Complete	…
		Mastcam	Z30 6 × 2 mosaic of Grimmauld Place slope	432	No	…	…	…	…	…	Complete	…
		Mastcam	ZCAM single frame of AEGIS target	36	No	…	…	…	…	…	Complete	…
		AEGIS (L/V/R)	Base of Grimmauld Place slope	184	No	…	…	…	Complete	…	…	…
	Heli	Survey inflight imager	High altitude (300 m)	900	No	…	…	…	…	…	…	300 m
		Oblique image	Ascent from site (Flutterby Bush)	48	No	…	…	…	…	…	Complete	…
		Oblique image	Descent to landing site (Cleansweep)	48	No	…	…	…	Complete	…	…	…
		Landed VISIR	Landing site (Cleansweep)	64	No	…	…	…	Complete	…	…	…
		Landed image	Landing site (Cleansweep)	48	No	…	…	…	…	…	Complete	…

Table D1
(Continued)

Planning Sol	Vehicle	Instrument	Activity/Target	Data Volume (kB)	Decisional Downlink on Sol Acquired	Sol Downlinked					End-of-exercise Downlink Pass	Remaining Onboard Indefinitely
						101	102	103	104	105		
103	Rover	Mastcam	Specialis Revelio 3 × 3 mosaic	3240	No	…	…	…	…	…	Complete	…
		XRF	Fizzing Whizbees	2.4	Yes	…	…	Complete	…	…	…	…
		XRF	Twilfitt_and_Tattings	2.4	Yes	…	…	Complete	…	…	…	…
		Turretcam	Fizzing Whizbees	144	No	…	…	…	…	…	Complete	…
		Turretcam	Twilfitt_and_Tattings	144	No	…	…	…	…	…	Complete	…
		RMI	Bludger	16	No	…	…	…	…	…	Complete	…
		RMI	Venomous_Tentacula	16	No	…	…	…	…	…	Complete	…
		VISIR	Bludger	80	Yes	…	…	Complete	…	…	…	…
		VISIR	Venomous_Tentacula	80	No	…	…	…	…	…	Complete	…
		LIBS	Bludger	80	Yes	…	…	Complete	…	…	…	…
		LIBS	Venomous_Tentacula	80	No	…	…	…	…	…	Complete	…
		Navcam	PDI 360 pano	160	Partial	…	…	180°	…	…	180°	…
		Mastcam	PDI mosaic of workspace	216	Yes	…	…	Complete	…	…	…	…
		Mastcam	AEGIS doc image	36	No	…	…	…	…	…	Complete	…
		AEGIS (L/V/R)	Rock in nearfield	184	Partial	…	…	IR	…	…	LIBS/RMI	…
	Heli	Survey inflight imager	Low altitude (128 m)	3072	No	…	…	…	…	…	64 m	64 m
		Survey inflight imager	High altitude (168 m)	504	No	…	…	…	…	…	Complete	…
		Oblique image	Imaging #1 at Godric's Hollow	48	No	…	…	…	Complete	…	…	…
		Oblique image	Imaging #2 toward Hogsmeade	48	No	…	…	…	Complete	…	…	…
		Oblique image	Imaging #3 at landing site Chizpurfle (west)	48	No	…	…	…	…	Complete	…	…
		Oblique image	Imaging #4 at landing site Chizpurfle (north)	48	No	…	…	…	…	…	Complete	…
		Oblique image	Imaging #5 at landing site Chizpurfle (east)	48	No	…	…	…	…	…	Complete	…
		Landed VISIR	Chizpurfle landing site	64	No	…	…	…	…	…	Complete	…
		Landed image	Chizpurfle landing site	48	No	…	…	…	…	…	Complete	…
104	Rover	Mastcam	Specialis Revelio M-100	288	Yes	…	…	…	Complete	…	…	…
		Turretcam	Bludger	144	Yes	…	…	…	Complete	…	…	…
		XRF	Bludger	2.4	Yes	…	…	…	Complete	…	…	…
		RAMAN	Bludger	9.6	Yes	…	…	…	Complete	…	…	…
		RAMAN	Fizzing Whizbees	9.6	Yes	…	…	…	Complete	…	…	…
		LIBS	Beauxbatons	80	Yes	…	…	…	Complete	…	…	…
		RMI	Beauxbatons	16	No	…	…	…	…	…	Complete	…
	Heli		Low altitude (147 m)	3528	No	…	…	…	…	…	Complete	…

Table D1
(Continued)

Planning Sol	Vehicle	Instrument	Activity/Target	Data Volume (kB)	Decisional Downlink on Sol Acquired	Sol Downlinked					End-of-exercise Downlink Pass	Remaining Onboard Indefinitely
						101	102	103	104	105		
		Survey inflight imager										
		Oblique image	Landing site (Bubotuber); west direction	48	No	…	…	…	…	…	Complete	…
		Landed image	Landing site (Bubotuber)	48	No	…	…	…	…	…	Complete	…
105	Rover	Mastcam	Beauxbatons M-100	36	Yes	…	…	…	…	Complete	…	…
		Navcam	PDI 270 pano	120	Yes	…	…	…	…	Complete	…	…
		Mastcam	Mid-drive M-30 3 × 2 mosaic toward Godric's Hollow and Bloody Baron	216	Yes	…	…	…	…	Complete	…	…
	Heli	Survey inflight imager	Low altitude (297 m)	7128	…	…	…	…	…	…	94 m	203 m
		Oblique image	Imaging #1 near Owlery	48	Yes	…	…	…	…	Complete	…	…
		Oblique image	Imaging #2 near Azkaban	48	Yes	…	…	…	…	Complete	…	…

Appendix E
Rover LIBS And XRF Results

Table E1 presents the normalized oxide abundances measured for the rover's LIBS and XRF targets.

Table E1
Rover LIBS and XRF Normalized Oxide Abundances

Sol	Measurement	Name	Al2O3 (%)	Al2O3 +/− (%)	CaO[a] (%)	CaO +/− (%)	FeO[b] (%)	FeO +/− (%)	K2O (%)	K2O +/− (%)	MgO (%)	MgO +/− (%)	MnO (%)	MnO +/− (%)	Na2O (%)	Na2O +/− (%)	SiO2 (%)	SiO2 +/− (%)	TiO2 (%)	TiO2 +/− (%)
100	LIBS	AEGIS 100	4.13	1.29	3.65	0.12	16.87	1.87	3.00	0.32	2.62	0.00	0.11	0.00	1.44	0.10	14.52	0.45	4.20	0.58
100	LIBS	AEGIS 100	0.00	4.42	3.46	0.08	13.29	1.02	1.97	0.15	2.62	0.00	0.10	0.00	1.04	0.04	14.62	0.15	3.97	0.17
100	LIBS	AEGIS 100	5.49	0.35	3.69	0.07	10.32	0.95	1.80	0.20	2.60	0.00	0.09	0.00	1.01	0.06	12.22	2.75	3.36	0.39
100	LIBS	AEGIS 100	3.76	1.68	3.59	0.10	11.34	2.02	1.72	0.22	2.62	0.00	0.11	0.00	1.21	0.08	14.26	0.30	3.44	0.63
100	LIBS	AEGIS 100	6.06	0.08	3.79	0.04	13.54	0.56	2.59	0.14	2.62	0.00	0.11	0.00	1.55	0.04	14.44	0.16	3.81	0.39
	LIBS weighted average and normalized for O	AEGIS 100	12.76	0.13	7.86	0.14	27.43	0.38	4.64	0.05	5.54	0.14	0.22	0.00	2.65	0.04	30.71	0.51	8.18	0.10
102	LIBS	Twillfit and Tattings	9.53	0.95	14.01	0.22	17.34	0.90	2.00	0.28	10.60	0.03	0.18	0.00	2.50	0.14	52.78	0.09	5.58	1.11
102	LIBS	Twillfit and Tattings	10.12	0.66	14.20	0.20	18.42	0.70	2.02	0.23	10.60	0.02	0.19	0.00	3.01	0.10	53.01	0.04	6.85	0.70
102	LIBS	Twillfit and Tattings	7.46	0.61	15.01	0.33	11.27	0.93	3.14	0.16	10.55	0.01	0.18	0.00	3.16	0.17	52.97	0.10	8.34	0.14
102	LIBS	Twillfit and Tattings	7.57	1.10	15.15	0.60	18.24	0.47	2.12	0.28	10.58	0.02	0.18	0.00	3.35	0.22	52.76	0.06	8.45	0.30
102	LIBS	Twillfit and Tattings	7.70	0.80	15.55	0.30	17.53	1.04	1.91	0.28	10.60	0.02	0.18	0.00	3.37	0.13	52.67	0.05	9.38	0.12
	LIBS weighted average and normalized for O	Twilfitt and Tattings	7.19	0.07	12.27	0.22	14.61	0.20	2.10	0.02	8.94	0.22	0.16	0.00	2.57	0.04	44.69	0.74	7.48	0.09
103	LIBS	Bludger	11.36	0.02	9.55	0.38	14.29	1.40	1.87	0.32	10.79	0.01	0.19	0.00	3.26	0.39	52.16	0.61	10.36	0.27
103	LIBS	Bludger	6.96	1.45	12.11	0.70	13.18	1.32	1.27	0.15	10.77	0.01	0.18	0.00	2.64	0.08	53.16	0.03	9.21	0.25
103	LIBS	Bludger	10.48	0.86	10.76	0.16	10.84	0.42	1.54	0.36	10.78	0.01	0.19	0.00	2.29	0.17	52.69	0.59	10.21	0.30
103	LIBS	Bludger	10.66	1.09	11.50	0.25	13.75	1.77	1.93	0.34	10.78	0.00	0.17	0.00	2.37	0.21	53.12	0.06	10.38	0.09
103	LIBS	Bludger	9.51	2.39	11.05	0.24	10.74	0.39	2.62	0.25	10.76	0.02	0.19	0.00	1.78	0.13	53.16	0.01	10.34	0.20
	LIBS weighted average and normalized for O	Bludger	10.15	0.10	9.75	0.17	9.92	0.14	1.51	0.02	9.64	0.24	0.17	0.00	2.14	0.03	47.53	0.79	9.18	0.11
103	LIBS	AEGIS 103	11.32	0.18	12.48	0.67	12.56	0.66	1.35	0.11	10.67	0.02	0.19	0.00	2.01	0.08	53.05	0.11	9.65	0.20
103	LIBS	AEGIS 103	0.00	6.90	8.92	0.42	30.64	0.68	2.52	0.28	10.79	0.01	0.20	0.00	2.69	0.17	51.66	0.97	9.50	0.32
103	LIBS	AEGIS 103	0.00	5.26	9.90	0.12	17.01	1.29	1.66	0.19	10.77	0.01	0.20	0.00	2.29	0.06	51.94	0.39	10.10	0.33
103	LIBS	AEGIS 103	9.60	0.87	9.69	0.27	10.87	0.25	1.63	0.16	10.74	0.01	0.19	0.00	2.09	0.07	50.59	1.17	5.24	1.75
103	LIBS	AEGIS 103	0.00	11.36	9.90	0.19	28.89	0.79	0.88	0.14	10.72	0.02	0.19	0.00	2.16	0.16	37.46	5.19	10.29	0.15
	LIBS weighted average and normalized for O	AEGIS 103	9.94	0.10	8.74	0.16	12.72	0.18	1.24	0.01	9.53	0.24	0.17	0.00	1.94	0.03	46.87	0.78	8.84	0.11

Table E1
(Continued)

Sol	Measurement	Name	Al2O3 (%)	Al2O3 +/− (%)	CaO[a] (%)	CaO +/− (%)	FeO[b] (%)	FeO +/− (%)	K2O (%)	K2O +/− (%)	MgO (%)	MgO +/− (%)	MnO (%)	MnO +/− (%)	Na2O (%)	Na2O +/− (%)	SiO2 (%)	SiO2 +/− (%)	TiO2 (%)	TiO2 +/− (%)
103	LIBS	Venemous Tentacula	8.98	2.25	11.98	0.41	15.98	1.01	1.02	0.17	10.58	0.03	0.19	0.00	2.04	0.08	53.01	0.14	4.36	0.85
103	LIBS	Venemous Tentacula	9.96	0.73	11.64	0.22	14.70	0.47	1.19	0.16	10.50	0.03	0.19	0.00	2.02	0.06	51.43	0.51	3.19	0.38
103	LIBS	Venemous Tentacula	8.97	0.93	11.19	0.12	16.43	0.58	1.02	0.12	10.56	0.03	0.19	0.00	1.98	0.04	51.11	0.81	4.81	0.45
103	LIBS	Venemous Tentacula	5.93	1.17	11.29	0.13	13.74	0.46	1.56	0.08	10.53	0.02	0.19	0.00	2.24	0.05	52.88	0.29	2.84	0.84
103	LIBS	Venemous Tentacula	10.73	0.49	11.37	0.28	15.85	0.43	1.42	0.16	10.60	0.02	0.19	0.00	2.24	0.08	53.03	0.08	2.74	0.53
	LIBS weighted average and normalized for O	Venemous Tentacula	9.18	0.09	10.58	0.19	14.14	0.20	1.25	0.01	9.87	0.24	0.18	0.00	1.94	0.03	49.50	0.82	3.36	0.04
103	APXS	Twilfit and Tattings	8.77	0.09	63.36	1.13	0.71	0.01	0.25	0.00	9.25	0.23	0.22	0.00	0.00	0.00	16.97	0.28	0.46	0.01
103	APXS	Fizzing Whizbees	21.45	0.21	1.92	0.03	1.75	0.02	2.27	0.02	5.61	0.14	0.02	0.00	0.00	0.00	66.72	1.11	0.26	0.00
104	LIBS	Beauxbatons	10.72	0.40	10.87	0.09	18.33	0.75	1.40	0.08	10.67	0.02	0.19	0.00	2.09	0.06	53.16	0.03	5.85	0.69
104	LIBS	Beauxbatons	0.00	5.67	10.30	0.30	25.58	1.33	2.41	0.60	10.62	0.03	0.20	0.00	2.32	0.10	33.72	14.64	8.76	0.64
104	LIBS	Beauxbatons	9.96	1.16	10.23	0.60	12.50	1.44	2.74	0.27	10.68	0.02	0.19	0.00	2.83	0.16	53.05	0.07	5.54	0.67
104	LIBS	Beauxbatons	10.39	0.91	10.97	0.38	15.75	0.68	1.50	0.13	10.63	0.02	0.19	0.00	2.24	0.06	52.97	0.17	5.19	0.82
104	LIBS	Beauxbatons	9.99	1.53	10.74	0.26	15.13	0.89	1.80	0.10	10.57	0.04	0.19	0.00	1.99	0.13	52.35	0.29	2.25	1.05
	LIBS weighted average and normalized for O	Beauxbatons	9.39	0.09	9.64	0.17	15.14	0.21	1.43	0.02	9.49	0.24	0.17	0.00	1.97	0.03	47.35	0.79	5.42	0.07
104	APXS	Bludger	12.31	0.12	47.11	0.84	0.78	0.01	1.20	0.01	0.00	0.00	1.00	0.01	0.00	0.00	37.55	0.62	0.06	0.00

Notes.
[a] Calcium values were abnormally high (9.6% Ca) for all LIBS calibrations.
[b] Iron values could erroneously imply values of up to 25% Fe if the contact between the laser aperture and target was not perfectly flat.

ORCID iDs

Kathryn M. Stack https://orcid.org/0000-0003-3444-6695
Samantha J. Gwizd https://orcid.org/0000-0001-5818-9123
Catherine D. Neish https://orcid.org/0000-0003-3254-8348
Brett B. Carr https://orcid.org/0000-0002-1033-3082
Christopher W. Hamilton https://orcid.org/0000-0001-9731-517X

References

Alibay, F., Koch, J., Verma, V., et al. 2022, On the Operational Challenges of Coordinating a Helicopter and Rover Mission on Mars, in 2022 IEEE Aerospace Conf. (Piscataway, NJ: IEEE), 1
Allwood, A. C., Wade, L. A., Foote, M. C., et al. 2020, PIXL: Planetary Instrument for X-ray Lithochemistry, SSRv, 216, 134
Anderson, J. L., Brown, T. L., Cacan, M., et al. 2024, Lessons from Ingenuity's Climb Up Jezero Crater Delta, in 2024 IEEE Aerospace Conf. (Piscataway, NJ: IEEE), 1
Anderson, J. L., Karras, J., Cacan, M., et al. 2023, Ingenuity, One Year of Flying on Mars, in 2023 IEEE Aerospace Conf. (Piscataway, NJ: IEEE), 1
Balaram, J., Aung, M., Golombek, M. P., et al. 2021, The Ingenuity Helicopter on the Perseverance Rover, SSRv, 217, 56
Bapst, J., Parker, T. J., Balaram, J., et al. 2021, Mars Science Helicopter: Compelling Science Enabled by an Aerial Platform, BAAS, 53, 361
Barnes, J. W., Turtle, E. P., Trainer, M. G., et al. 2021, Science Goals and Objectives for the Dragonfly Titan Rotorcraft Relocatable Lander, PSJ, 2, 130
Bateman, K. M., Williams, R. T., Shipley, T. F., et al. 2022, Strategies for Effective Unmanned Aerial Vehicle Use in Geological Field Studies Based on Cognitive Science Principles, Geosp, 18, 1958
Bell, J. F., III, Godber, A., McNair, S., et al. 2017, The Mars Science Laboratory Curiosity Rover Mastcam Instruments: Preflight and In-flight Calibration, Validation, and Data Archiving, E&SS, 4, 396
Bell, J. F., Maki, J. N., Mehall, G. L., et al. 2021, The Mars 2020 Perseverance Rover Mast Camera Zoom (Mastcam-z) Multispectral, Stereoscopic Imaging Investigation, SSRv, 217, 24
Bhartia, R., Beegle, L. W., DeFlores, L., et al. 2021, Perseverance's Scanning Habitable Environments with Raman and Luminescence for Organics and Chemicals (Sherloc) Investigation, SSRv, 217, 58
Brockers, R., Proença, P., Delaune, J., et al. 2022, On-board Absolute Localization Based on Orbital Imagery for a Future Mars Science Helicopter, in 2022 IEEE Aerospace Conf. (Piscataway, NJ: IEEE), 1
Calef, F. J., III, Soliman, T. K., Roberts, J., et al. 2023, Mapping Operations, Spatial Products, and Map Services for the Mars 2020 Perseverance Rover, LPICo, 2991, 7037
Calef, F. J., III, Soliman, T. K., Roberts, J., et al., 2024 MMGIS (Multi-mission Geographic Information System), GitHub, https://nasa-ammos.github.io/MMGIS
Carr, B. B., Varnam, M., Hadland, N., et al. 2024, Evaluating the Use of Unoccupied Aircraft Systems (Uass) for Planetary Exploration in Mars Analog Terrain, PSJ, 5, 231
Cheng, L., Spanovich, N., Vaughan, A., et al. 2008, Opposite Ends of the Spectrum: Cassini and Mars Exploration Rover Science Operations, in 2008 SpaceOps Conf (Reston, VA: AIAA), 1
Diblee, T. W. 1968, Geology of the Fremont Peak and Opal Mountain Quadrangles, Bulletin 188 (Sacramento, CA: California Geological Survey Publications)
Edgett, K. S., & Sarkar, R. 2021, Recognition of Sedimentary Rock Occurrences in Satellite and Aerial Images of Other Worlds—insights from Mars, RemS, 13, 4296
Edgett, K. S., Yingst, R. A., Ravine, M. A., et al. 2012, Curiosity's Mars Hand Lens Imager (MAHLI) Investigation, SSRv, 170, 259
Fergason, R. L., Hare, T. M., Mayer, D. P., et al. 2020, Mars 2020 Terrain Relative Navigation Flight Product Generation: Digital Terrain Model and Orthorectified Image Mosaics, LPSC, 51, 2020
Francis, R., Estlin, T., Doran, G., et al. 2017, AEGIS Autonomous Targeting for Chemcam on Mars Science Laboratory: Deployment and Results of Initial Science Team Use, SciRobot, 2, 7
Francis, R., Williford, K., Stack, K. M., et al. 2018, The ROASTT-2017 Training Exercise for the Mars 2020 Science Team, LPSC, 49, 2588
Gellert, R., & Clark, B. C. 2015, In Situ Compositional Measurements of Rocks and Soils with the Alpha Particle X-Ray Spectrometer on NASA's Mars Rovers, Eleme, 11, 39
Grip, H. F., Conway, D., Lam, J., et al. 2022, Flying a Helicopter on Mars: How Ingenuity's Flights Were Planned, Executed, and Analyzed, in 2022 IEEE Aerospace Conf. (Piscataway, NJ: IEEE), 1
Gwizd, S., Stack, K. M., Francis, R., et al. 2024, Comparing Rover and Helicopter Planetary Mission Architectures in a Mars Analog Setting in Iceland, PSJ, 5, 172
Hamilton, C. W., Voigt, J. & The RAVEN Team 2023, The Rover-Aerial Vehicle Exploration Network (RAVEN): Field-testing The Next Generation of Mars Mission Design in Iceland, IAVCEI 2023 Scientific Assembly, ed. U. Kueppers, 1472
Heverly, M., Matthews, J., Lin, J., et al. 2013, Traverse Performance Characterization for the Mars Science Laboratory Rover, J. Field Robotics, 30, 835
Horn, B. K. P. 1981, Hill Shading and the Reflectance Map, IEEEP, 69, 14
Khan, S. Y., Stack, K. M., Yingst, R. A., et al. 2022, Characterization of Clasts in the Glen Torridon Region of Gale Crater Observed by the Mars Science Laboratory Curiosity Rover, JGRE, 127, 11
Kodikara, G. R., McHenry, L. J., Hynek, B. M., et al. 2024, Mapping Paleolacustrine Deposits with a UAV-borne Multispectral Camera: Implications for Future Drone Mapping On Mars, PSJ, 5, 265
Lang, N. P., Fedo, C. M., & Whisner, S. C. 2011, Terrestrial Analogs in the Mojave Desert of the Southwestern United States for Volcanic, Sedimentary, and Tectonic Processes on Other Planets, in Analogs for Planetary Exploration, ed. W. B. Garry & J. E. Bleacher, 483 (Boulder, CO: Geological Society of America), 465
Maki, J., Thiessen, D., Pourangi, A., et al. 2012, The Mars Science Laboratory Engineering Cameras, SSRv, 170, 77
Maki, J. N., Gruel, D., McKinney, C., et al. 2020, The Mars 2020 Engineering Cameras And Microphone on the Perseverance Rover: A Next-generation Imaging System for Mars Exploration, SSRv, 216, 137
Maki, J., Golombek, M., Ayoub, F., et al. 2024, Ingenuity Mars Helicopter Cameras: Description and Results, in Tenth Int. Conf. on Mars, 3479
Maurice, S., Wiens, R. C., Bernardi, P., et al. 2021, The SuperCam Instrument Suite on the Mars 2020 Rover: Science Objectives and Mast-unit Description, SSRv, 217, 47
Maurice, S., Wiens, R. C., Saccoccio, M., et al. 2012, The Chemcam Instrument Suite on the Mars Science Laboratory (MSl) Rover: Science Objectives and Mast Unit Description, SSRv, 170, 95
McEwen, A. S., Eliason, E. M., Bergstrom, J. W., et al. 2007, Mars Reconnaissance Orbiter's High Resolution Imaging Sciece Experiment (HiRISE), JGRE, 112, E05S02
Milkovich, S. M., Stack, K. M., Sun, V. Z., et al. 2022, Balancing Predictive and Reactive Science Planning for Mars 2020 Perseverance, in 2022 IEEE Aerospace Conf. (AERO) (Piscataway, NJ: IEEE), 1
Mishkin, A. H., Limonadi, D., Laubach, S. L., et al. 2006, Working the Martian Night Shift—the MER Surface Operations Process, ITRA, 13, 46
Moores, J. E., Francis, R., Mader, M., et al. 2012, A Mission Control Architecture for Robotic Lunar Sample Return as Field Tested in an Analog Deployment to the Sudbury Impact Structure, AdSpR, 50, 1666
National Academies of Sciences, Engineering, and Medicine 2023, Origins, Worlds, and Life: A Decadal Strategy for Planetary Science and Astrobiology 2023–2032 (Washington, DC: The National Academies Press)
Osinski, G. R., Battler, M. B., Caudill, C. M., et al. 2019, The Canmars Mars Sample Return Analog Mission, P&SS, 166, 110
Sun, V. Z., Hand, K. P., Stack, K. M., et al. 2023, Overview and Results from the Mars 2020 Rover's First Science Campaign on the Jezero Crater Floor, JGRE, 128, e2022JE007613
Sun, V. Z., Sholes, S., Stack, K. M., et al. 2024, Evolution of the Mars 2020 Perseverance Rover's Strategic Planning Process, in 2024 IEEE Aerospace Conf. (AERO) (Piscataway, NJ: IEEE), 1
Swan, R. M., Atha, D., Leopold, H., et al. 2021, AI4Mars: A Dataset for Terrain-aware Autonomous Driving on Mars, 2021 IEEE/CVF CVPRW (Piscataway, NJ: IEEE), 1982
Treiman, A. H., Filiberto, J., & Rivera-Valentín, E. G. 2020, How Good Is "Good Enough?" Major Element Chemical Analyses of Planetary Basalts by Spacecraft Instruments, PSJ, 1, 65
Tzanetos, T., Aung, M., Balaram, J., et al. 2022, Ingenuity Mars Helicopter: from Technology Demonstration to Extraterrestrial Scout, in 2022 IEEE Aerospace Conf. (AERO) (Piscataway, NJ: IEEE), 1
Vasavada, A. R. 2022, Mission Overview and Scientific Contributions from the Mars Science Laboratory Curiosity Rover after Eight Years of Surface Operations, SSRv, 218, 14
Verma, V., Maimone, M. W., Gaines, D. M., et al. 2023, Autonomous Robotics Is Driving Perseverance Rover's Progress on Mars, SciRobot, 8, 80

Verma, V., Nash, J., Saldyt, L., et al. 2024, Enabling Long & Precise Drives for the Perseverance Mars Rover via Onboard Global Localization, in 2024 IEEE Aerospace Conf. (Piscataway, NJ: IEEE), 1

Withrow-Maser, S., Johnson, W., Young, L. A., et al. 2021, Mars Science Helicopter: Conceptual Design of the Next Generation of Mars Rotorcraft, in AIAA ASCEND 2020 Conf. (Reston, VA: AIAA), 1

Woodburne, M. O., Tedford, R. H., & Swisher, C. C., III 1990, Lithostratigraphy, Biostratigraphy, and Geochronology of the Barstow Formation, Mojave Desert, Souther California, GSAB, 102, 459

Yingst, R. A., Bartley, J. K., Chidsey, T. J., et al. 2020, Is a Linear or a Walkabout Protocol More Efficient When Using a Rover to Choose Biologically Relevant Samples in a Small Region of Interest, AsBio, 20, 327

Yingst, R. A., Bartley, J. K., Cohen, B. A., et al. 2022, Using Rover-analogous Methodology to Discriminate between Volcanic and Sedimentary Origins in Successions Dominated by Igneous Composition, PSJ, 3, 240

Yingst, R. A., Cropper, K., Gupta, S., et al. 2016, Characteristics of Pebble and Cobble-sized Clasts along the Curiosity Rover Traverse from sol 100 to 750: Terrain Types, Potential Sources, and Transport Mechanisms, Icar, 280, 72

Yingst, R. A., Crumpler, L. H., Farrand, W. H., et al. 2010, Constraints on the Geologic History of "Home Plate" Materials Provided by Clast Morphology and Texture, JGRE, 115, E00F13

Yingst, R. A., Kah, L. C., Palucis, M., et al. 2013, Characteristics of Pebble- and Cobble-sized Clasts along the Curiosity Rover Traverse from Bradbury Landing to Rocknest, JGRE, 118, 11

Young, E., Yang, G., Wagner, T., et al. 2023, Relay Planning in the Perseverance Rover's First 600 Solar Days on Mars, in 2023 IEEE Aerospace Conf. (AERO) (Piscataway, NJ: IEEE), 1

Young, L. A., Lee, P., Aiken, E., et al. 2021, The Future of Rotorcraft and Other Aerial Vehicles for Mars Exploration, 77th VFS Annual Forum, ed. H. Kang & M. J. Duffy, (Fairfax, VA: The Vertical Flight Society)